Title: Effect of slag composition on H_2 generation and magnetic precipitation from molten steelmaking slag-steam reaction

Authors: JUNCHENG LI, DEBASHISH BHATTACHARJEE, XIAOJUN HU, DIANWEI ZHANG, SEETHARAMAN SRIDHAR and ZUSHU LI

Mailing address: WMG, University of Warwick, Coventry, CV4 7AL UK

E-mail: leejc2011@163.com

Corresponding author: ZUSHU LI

Contact e-mail: z.li.19@warwick.ac.uk

JUNCHENG LI, formerly Research Fellow with WMG, the University of Warwick, Coventry, CV4 7AL, UK, is now Professor with School of Material Science and Engineering, Jiangsu University, Zhenjiang, Jiangsu Province, 212013 China. DEBASHISH BHATTACHARJEE, Global R&D Director, is with Tata Steel Research & Development, Moorgate, Rotherham, South Yorkshire, S60 3AR UK. XIAOJUN HU, Professors, is with the State Key Laboratory of Advanced Metallurgy, University of Science and Technology Beijing, Beijing 100083, P.R. China. DIANWEI ZHANG, Principal Researcher, is with Shougang Research Institute of Technology (Technical Centre), Shijingshan District, Beijing 100043. P. R. China. SEETHARAMAN SRIDHAR, formerly Tata Steel/RAEng Research Chair in Low Carbon Materials Technology with WMG, the University of Warwick, Coventry, CV4 7AL, UK, is now Professor with Department for Metallurgical and Materials Engineering, Colorado School of Mines, Golden, CO 80401, USA. ZUSHU LI, EPSRC Fellow in Manufacturing, is with WMG, the University of Warwick, Coventry, CV4 7AL, UK. Contact e-mail: z.li.19@warwick.ac.uk.

ABSTRACT

In this paper, the effect of slag composition (slag basicity CaO/SiO_2 and FeO concentation) on the amount of H_2 gas and magnetic spinel phase precipitated as a result of the reaction between synthetic steelmaking slag and steam at 1873 K (1600 °C) was studied by thermodynamic simulation (using Thermodynamic Package FactSage 7.0) and laboratory experiments. The thermodynamic calculation showed that, with increasing slag basicity (CaO/SiO_2) from 1.0 to 2.5, for 100 g slags reacting with 100 g H_2O gas, the accumulated amount of the produced H_2 gas increased from 0.17 g to 0.27 g, while the amount of magnetic spinel phase first increased and then decreased, with the maximum of 16.71g at the basicity of 1.5. When the FeO concentration increased from 15% to 30% for the slag with basicity of 2.0, the accumulated amount of the produced H_2 gas increased from 0.17 g to 0.28 g, and the amount of magnetic spinel phase increased from 5.88 g to 10.59 g. The laboratory experiments were conducted in confocal laser scanning microscope to verify the reaction between 0.2 g slag and 3.75 l H_2O-Ar gas ($P_{H_2O} = 0.2atm$). The results indicated that, for 100 g slags, with increasing slag basicity (CaO/SiO_2) from 1.0 to 2.5, both the produced H_2 gas and magnetic spinel phase first increased and then decreased, with the maximum of 0.09 g gas and 37.00 g magnetic spinel phase at the slag basicity of 1.50. For the FeO concentration increasing from 15% to 30%,

the amount of both the produced H_2 gas and magnetic spinel phase increased from 0.04 g to 0.10 g and from 18.00 g to 27.00 g respectively. The reaction rate between molten CaO-SiO_2-FeO-MnO-Al_2O_3-MgO slag and the moisture ($P_{H_2O} = 0.2atm$) increased with increasing FeO activity in the slag. The dependence of the reaction rate (mol/cm^2/second) on FeO content can be expressed as $r = (7.67(a_{FeO}) - 2.99) \times 10^{-7}$.

Keywords: steelmaking slag; moisture, H_2 gas; spinel; basicity; reaction

I. INTRODUCTION

Steel slag is a by-product from the steelmaking process. Although the steel slag composition varies with steelmaking furnace type, steel grades made and pre-treatment method, the main components in steel slag are CaO, SiO_2, FeO (Fe_2O_3) with certain amount of Al_2O_3, MgO, MnO and P_2O_5. [1, 2] The molten steelmaking slag, in the temperature range of 1723 - 1923 K (1450-1650 °C) contains substantial amount of high quality thermal energy. Researchers have been exploiting various chemical methods to recover the waste heat, including methane reforming [3, 4], coal and biomass gasification [5-8], and direct compositional modification of slags [9-11]. During the heat recovery by using chemical methods, slags can act as not only heat carriers but also catalysts and reactants, which expands the field of slag utilization. However, due to existing gaps in knowledge, the industrial deployment of these energy recovery methods

is some way off. These include managing the low thermal conductivity of slags [12, 13], kinetics of crystallization [14, 15] and discontinuous availability [16, 17].

Besides the high-temperature waste heat, the slag contains valuable material. Taking into account 15%-35% of FeO in the steelmaking slag and about 114 Mt BOS (Basic Oxygen Steelmaking) process slag generated worldwide in 2013 [18], it is extremely important to develop efficient solutions to recover valuable materials from slags that could be utilized as raw materials including for sintering mixture or for pelletizing iron ores. Several carbothermal reduction methods [19-21] have been developed to recycle iron from steelmaking slags. However, its implementation is constrained by unavoidable carbon footprint and large energy consumption. A sustainable approach to utilize steelmaking slag components based on transformation of non-magnetic iron monoxide to magnetite by oxidation has been investigated by Semykina et al. [22-24]. In this process, air could be used to produce an oxidizing atmosphere to transform FeO into magnetite, followed by a magnetic separation of magnetite from the pre-treated slag. The rest of the slag (non-magnetic) could be effectively used in production of cement binder or in other applications.

Bhattacharjee *et al.* [25] and Mukherjee and Bhattacharjee [26] sprayed water on molten slag, and subsequently thermo-chemical decomposition

of steam took place on the slag surface, resulting in the generation of H_2. With regards to the steam-slag process for the generation of hydrogen gas, Matsuura *et al.* [27] predicted the effects of slag temperature, slag composition, gas temperature and partial pressure of H_2O on production behavior of H_2 gas by FactSage calculation. Accordingly, Sato *et al.* [28] designed experiments to realize this reaction.

The current authors are aiming to develop a novel process to recover both the thermal heat and valuable materials from the molten slag by reacting molten slag with steam. As the continuation of our previous study [18], this paper studies the effect of slag composition (slag basicity CaO/SiO_2 and FeO concentration) on the H_2 generation during the reaction and the precipitation of magnetic spinel phase from the slag after the slag-steam reactions. BOS slags comprise major components of CaO, SiO_2 and FeO (totalling more than 80 mass%) and minor components of MgO, Al_2O_3, MnO and P_2O_5. Hence, the main components of basicity (CaO/SiO_2 ratio) and FeO concentration on the production of H_2 gas and the generation of magnetically susceptible compounds in the reaction between molten slag and water vapor are studied in this work. The reaction mechanism and reaction rate have also been investigated.

II. EXPERIMENTAL

A. Slag Samples

The composition of the synthesized slag samples characterized by XRF (XRF-1800X from Shimadzu Corporation) in the present study are listed in **Table 1**. As the main components of steelmaking slag are CaO, SiO_2 and FeO, with small amount of Al_2O_3, MgO and MnO, as a result, for all the slags, the compositions of Al_2O_3, MgO and MnO were kept constant at 5.0 mass%, respectively. Slags #1 to #4 were prepared to study different bacisities (CaO/SiO_2 ratios) in the range of 1.0 to 2.5, while slags #5, #6, #3 and #7 were used to study the effect of FeO concentration in the slags.

All the slags were made from chemical reagents of CaO, SiO_2, FeO, MnO, Al_2O_3 and MgO, with a purity of 99.9 wt.%, supplied by Sigma Aldrich. Prior to mixing, the chemical reagents of CaO and SiO_2 were dried at 1273 K (1000 °C) for 4 hours under Ar atmosphere to remove the small amount of volatiles and hydrones. The dry chemical reagent powders were well mixed with FeO and MnO powders based on Table 1, then placed into a platinum crucible, and heated in a tube furnace at 1873 K (1600 °C) for 2 hours under high purity of Ar atmosphere to homogenize the slags. Finally, the molten slag was rapidly cooled to room temperature under high purity of Ar atmosphere and the slag achieved in this process was called pre-melted slag. The temperature of the tube furnace in this study was controlled by a program controller with an R type thermocouple, within the observed precision range of ±3 K.

B. Experimental Apparatus and Procedure

Figure 1 shows a schematic diagram of the experimental apparatus,

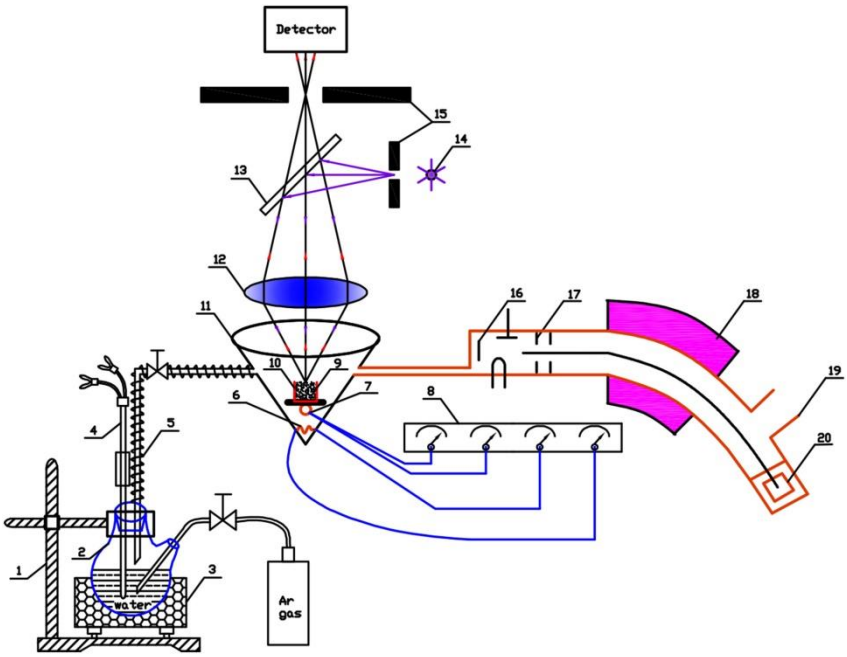

Figure 1 Schematic diagram of experimental apparatus: 1. Retort stand; 2. Round-bottom flask; 3. Heating mantles; 2. Temperature probe; 5. Heater tape; 6. Halogen lamp; 7.Thermocouple; 8. Temperature controller; 9. Samples; 10. Platinum crucible; 11. Furnace chamber; 12. Lens; 13. Beam splitter; 14. He-Ne laser; 15. Pin hole; 16. Ion source; 17. Accelerating voltage; 18. Electromagnet; 19. Vacuum pump; 20. Detector

which mainly consists of the moisture generator, high temperature confocal laser scanning microscope (CLSM) and mass spectrometry. The details of the moisture generator and the CLSM have been described in the previous publication [18], and the mass spectrometry (HPR-20 QIC from Hiden Analytical), with the scanning cycle of 12 s, was employed to

analyze the real-time gas composition of H_2, Ar, O_2 and H_2O from the off-gas of the reaction chamber. Prior to each experiment, 0.2 g of the pre-melted slag was placed into a Pt crucible and then heated at the hot stage of CLSM under Ar atmosphere. To ensure the slag fully melted, the sample was kept at 1873 K (1600 °C) under argon gas for 5 minutes and then the argon gas was switched to H_2O-Ar gas (with the Ar gas rate of 300 ml/min and H_2O partial pressure of approximately 0.2 atm) to react with molten slag for around 10 minutes at 1873 K (1600 °C), which was equal to 3.75 l H_2O-Ar gas ($P_{H_2O} = 0.2atm$) introduced into CLSM during the reaction. After the reaction, the H_2O-Ar gas was switched to Ar gas and the slag was cooled at a fixed cooling rate of 10 K/min. The mineral composition of the cooled slags was analyzed by XRD (Empyrean from Panalytical).

Parallel experiments were carried out under Ar atmosphere only, that is, the molten slag was held under Ar gas (instead of reacting with H_2O-Ar gas) at 1873 K (1600 °C) for 10 minutes. All the other experimental procedures are exactly similar. The samples obtained in the experiment of reacting with H_2O-Ar gas are thereafter labelled as “Reacted” slags, while the samples obtained in the parallel experiments (without reacting with H_2O-Ar gas) are labelled as “Un-reacted” slags.

III. RESULTS

A. Thermodynamic simulation of H_2 generation and precipitated phases

Thermodynamic calculations by using FactSage 7.0 with databases of FactPS and FToxid were conducted to predict the amount of H_2 generated during the reaction and the precipitated phases during the cooling for both the un-reacted (in Ar) and reacted (in moist) slags with different slag compositions as listed in Table 1. The calculations comprised three steps. The first step of calculation is for slag melting in Ar, that is, 100 g of synthetic slag was equilibrated at 1600 ℃ under Ar atmosphere in order to start with a homogenous molten phase. Step two is for slag-gas equilibrium, that is, 100 g of molten slag from the first step was equilibrated with H_2O-Ar gas (100 g, 100°C) resulting in condensed phases and H_2-H_2O-Ar gas. Finally, the reacted molten slag and condensed phases from step two were cooled under Ar atmosphere to calculate different phases precipitated in the cooled slags including magnetically susceptible compounds. The methodology of thermodynamic calculations has been described in detail in the previous publication. [18]

The calculation results show that when the molten slags as listed in the Table 1 were equilibrated with the inert Ar atmosphere at 1873 K (1600 °C), no H_2 gas was generated. However, when the slags were equilibrated

with the moist atmosphere at 1873 K (1600 °C), the accumulated H_2 gas generated increased not only with increasing the mass of H_2O introduced, but also with increasing the slag basicities (CaO/SiO_2) from 1.0 to 2.5 (**Figure 2**) and FeO concentration from 15% to 30% (**Figure 3**).

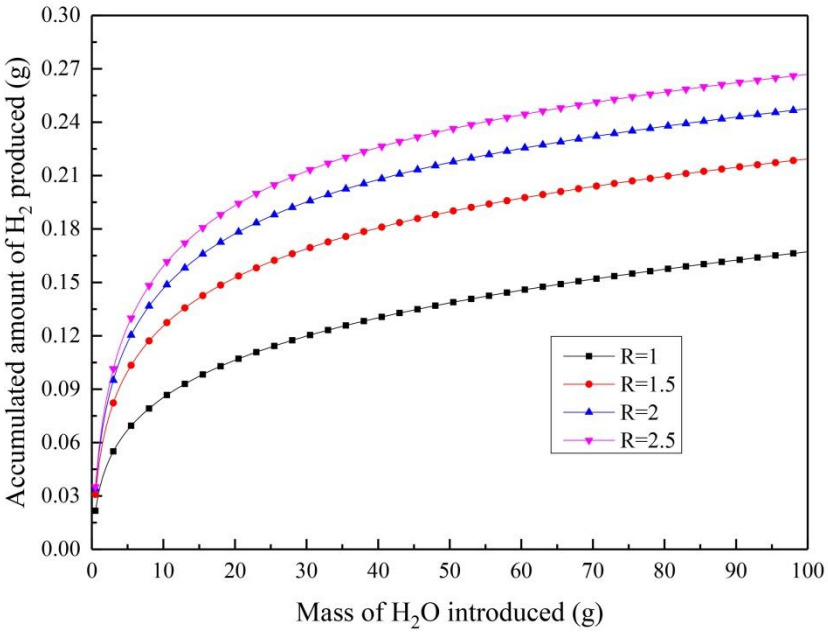

Figure 2 Change in the accumulated amount of H_2 gas produced as a function of the mass of H_2O introduced at different slag basicities

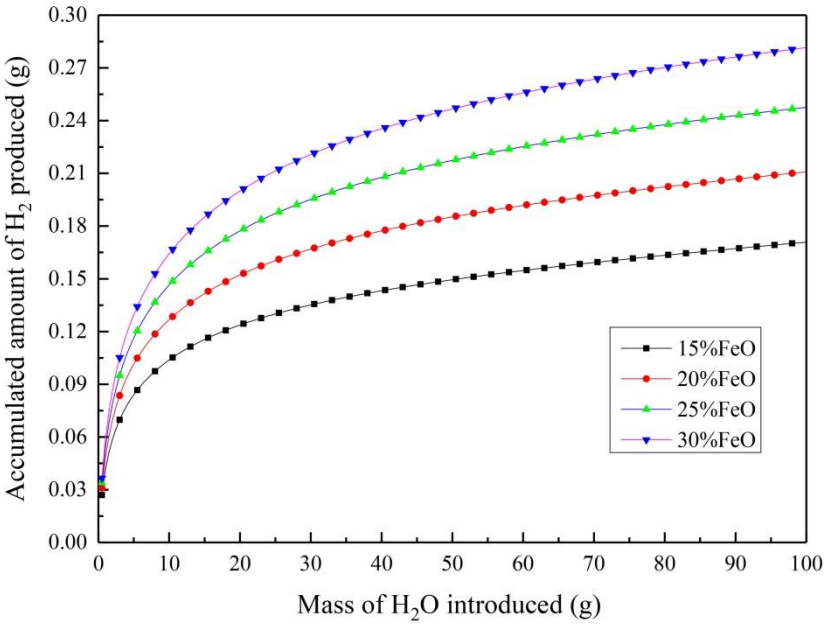

Figure 3 Change in the accumulated amount of H_2 gas produced as a function of the mass of H_2O introduced at different FeO concentrations

Figure 4 shows the calculated amount of different phases present in the

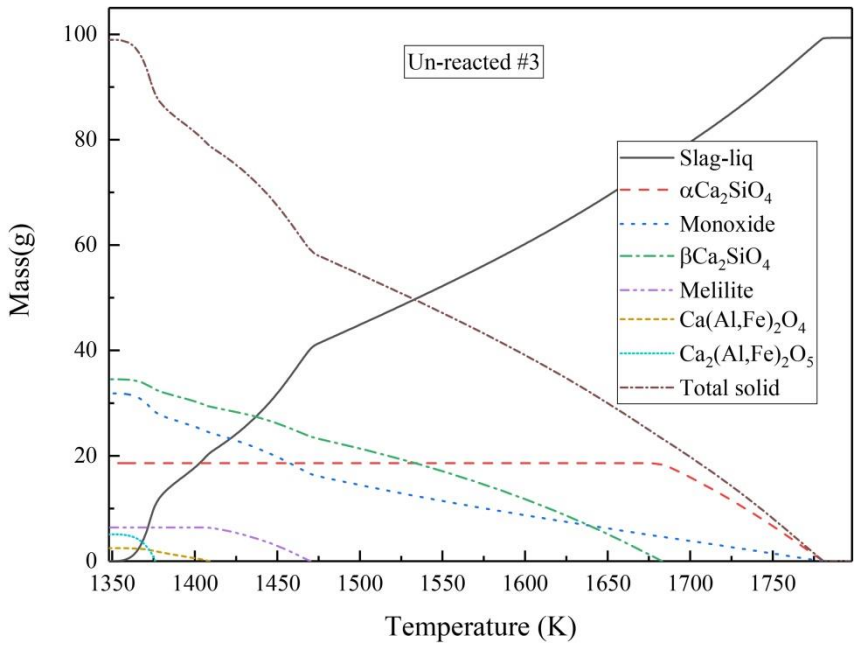

Figure 4 Change in the total amount of different phases precipitated from un-reacted slag #3

slag (CaO/SiO_2=2.0) during solidification after equilibrium with the Ar gas at 1873 K (1600 °C) (i.e. un-reacted slag). The precipitation sequence of phases was in the descending order of α-Ca_2SiO_4, monoxide, β-Ca_2SiO_4, melilite, $Ca(Al, Fe)_2O_4$ and $Ca_2(Al, Fe)_2O_5$, with the starting precipitation temperatures of 1781 K (1508 °C), 1780 K (1507 °C), 1683 K (1410 °C), 1470 K (1197 °C), 1409 K (1136 °C) and 1376 K (1103 °C) respectively. The slag-liquid completely solidified at 1364 K (1091 °C). In comparison, when the slag (with same CaO/SiO_2) was solidified after

being equilibrium with the moist gas at 1873 K (1600 °C) (i.e. reacted slag) (**Figure 5)**, the

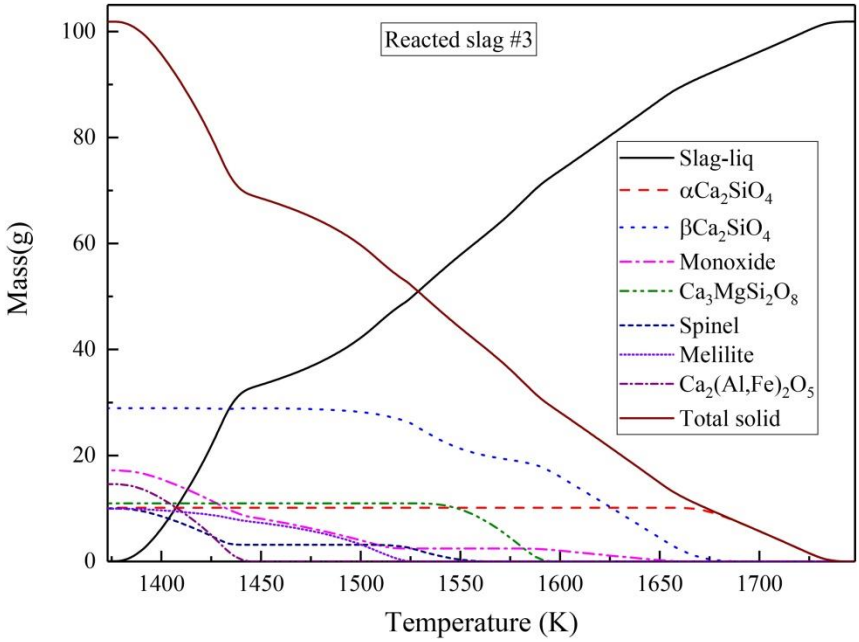

Figure 5 Change in the total amount of different phases precipitated from reacted slag #3

precipitation sequence of phases was in the descending order of α-Ca_2SiO_4, β-Ca_2SiO_4, monoxide, $Ca_3MgSi_2O_8$, spinel, melilite and $Ca_2(Al, Fe)_2O_5$, with the starting precipitation temperatures of 1734 K (1461 °C), 1673 K (1400 °C), 1657 K (1384 °C), 1589 K (1316 °C), 1548 K (1275 °C), 1524 K (1251 °C) and 1441 K (1168 °C) respectively. The slag-liquid completely solidified at 1391 K (1118 °C). The metal monoxides in both the un-reacted and reacted slags were the solid solution of FeO-MnO-MgO-(CaO-Fe_2O_3), with FeO accounting for more than 60%, while the melilite phase was mainly solid solution of $Ca_2AlSi_2O_7$ and $Ca_2Al_3O_7$. The spinel phase was only formed in the moist

gas and its constitution is presented in **Figure 6**. The spinel phase consists of 64.53% Fe_3O_4 and

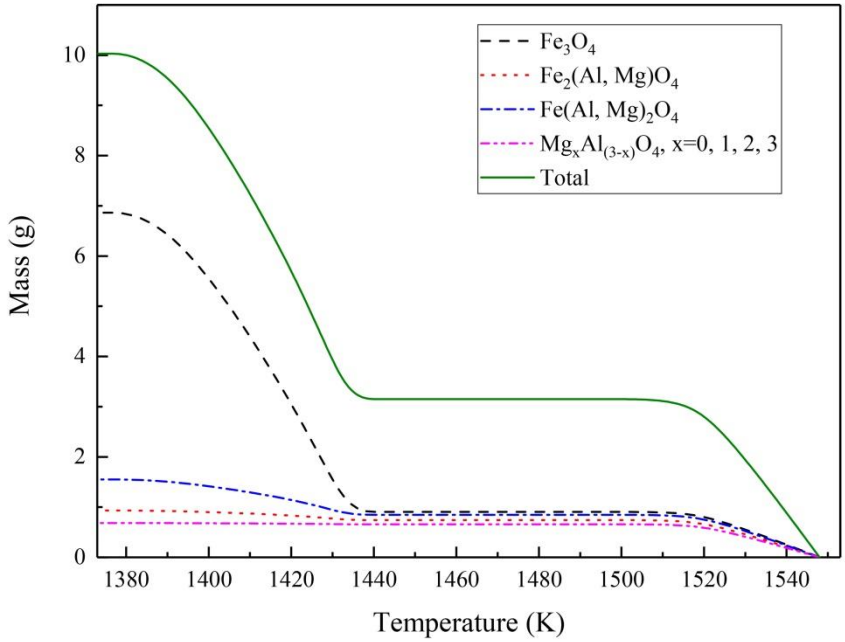

Figure 6 Constituents of spinel phase generated in the reacted slag #3

the rest of MgO-Fe_2O_3/Al_2O_3 and is labelled as magnetic spinel phase. **Figure 7** and **Figure 8** show the change in the accumulated amount of the

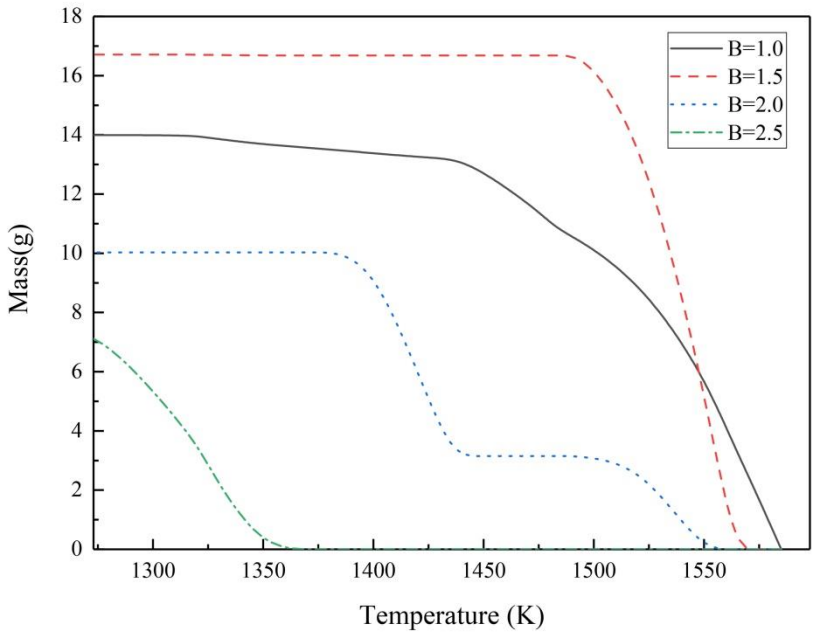

Figure 7 Change in the accumulated amount of spinel phase precipitated from reacted slags with different basicities

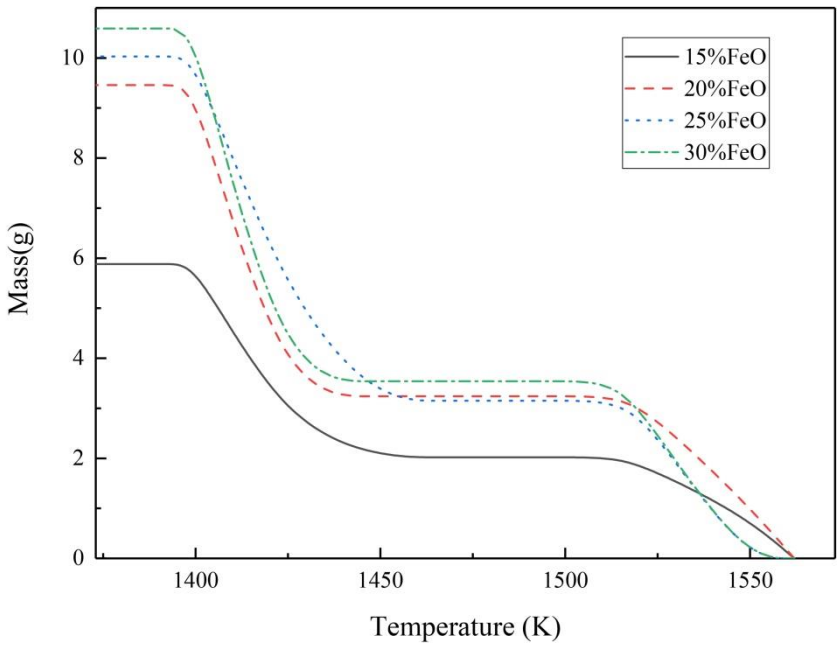

Figure 8 Change in the accumulated amount of spinel phase precipitated from reacted slags with different FeO concentrations

magnetic spinel phase precipitated from the reacted slags with slag basicity from 1.0 to 2.5 and FeO concentration from 15% to 30% respectively. As listed in **Table 2**, the amount of the magnetic spinel phase of the reacted slags first increases from 13.99 g to 16.71 g with increasing the slag basicity from 1.0 to 1.5 and then decreases to 10.03 g and 7.39 g with the slag basicity further increasing to 2.0 to 2.5. As the FeO concentration increases from 15% to 30%, the amount of spinel phase increases from 5.88 g to 10.59 g. In addition, the other Fe^{3+} containing phase ($Ca_2(Al, Fe)_2O_5$) begins to precipitate from the slags

with slag basicity equal to or above 2.0 and its amount increases with the increasing of slag basicity and FeO concentration.

B. H_2 generation behavior characterized by mass spectrometry

Figure 9 and **Figure 10** show typical gas composition for unreacted slag- and reacted slag (slag 3#) as determined by the mass spectrometer.

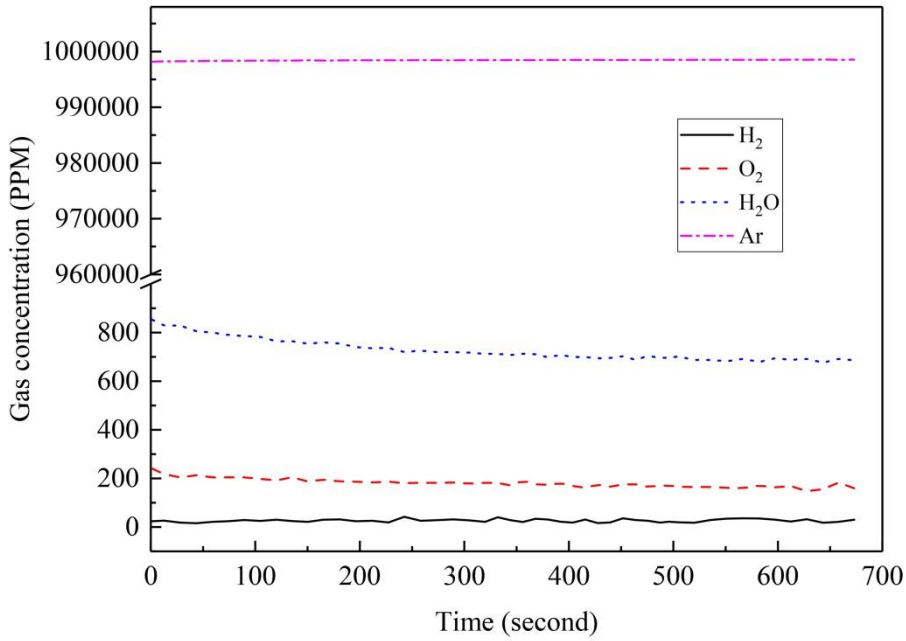

Figure 9 Gas composition for the unreacted slag as determined by mass spectrometry

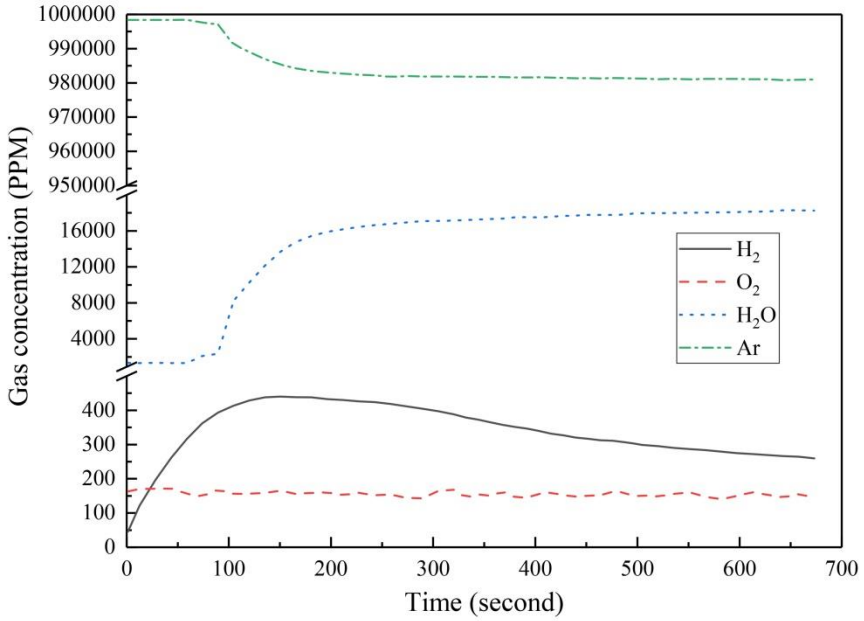

Figure 10 Gas composition for the reacted slag (slag 3#) as determined by mass spectrometry

As for the unreacted slag (Figure 9), there is a negligible change of gas composition with the progress of the parallel experiments, with the Ar accounting for 99.86% of the gases. It should be pointed out that on average oxygen partial pressure of 2.62×10^{-5} Pa and 26 ppm H_2 were detected in the parallel experiments. As for the reacted slag (Figure 10), with introducing H_2O, H_2 concentration in the generated gas firstly increased and then decreased, while the O_2 concentration kept the same during the reaction.

In order to investigate the effect of reactive moist atmosphere on the H_2 generation, the H_2 concentration in the parallel experiments will be deducted from the off-gas composition from the slag-steam reactions.

Figure 11 shows the change of accumulated H_2 gas in the moist atmosphere as a

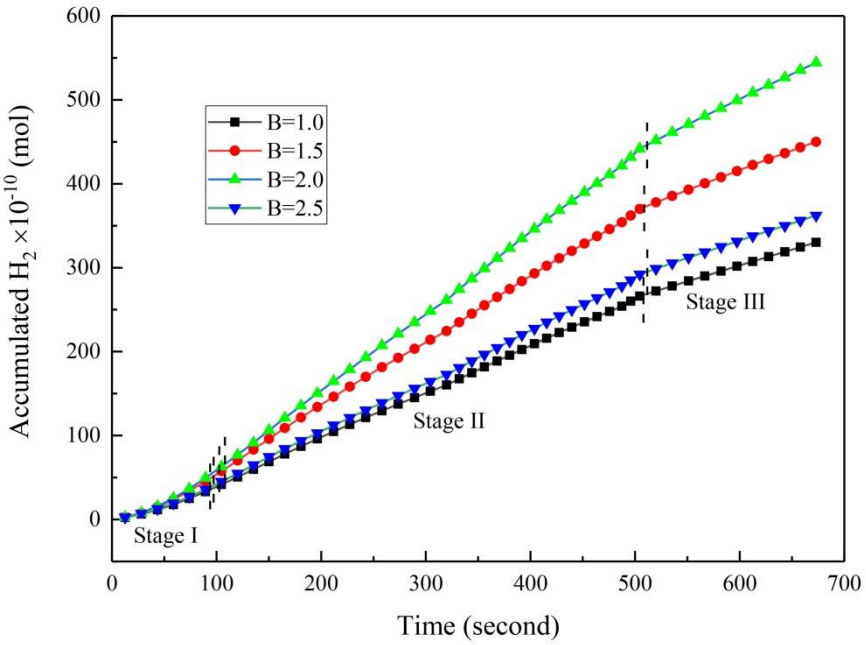

Figure 11 Changes of accumulated H_2 as a function of reaction time for slags with different basicities

function of reaction time for slags with different basicities from 1.0 to 2.5. The rate of H_2 gas evolution rapidly increased, reaching its maximum value after 120 seconds, and then gradually decreased. The change in accumulated H_2 gas during the reactions also showed a similar dependence with reaction time for the FeO concentration varying from 15% to 30% (**Figure 12)**.

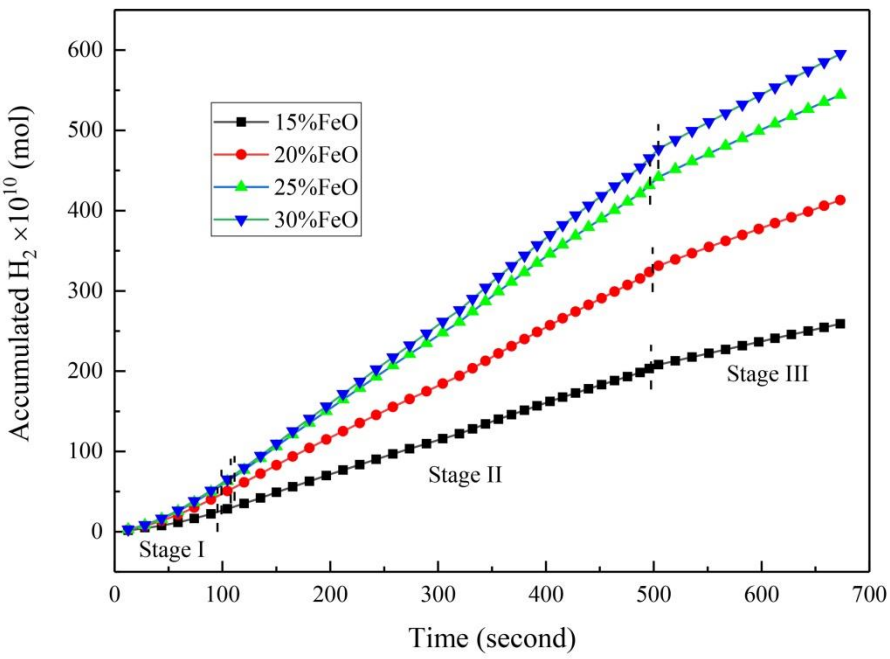

Figure 12 Changes of accumulated H_2 as a function of reaction time for slags with different FeO concentrations

According to the slope of accumulated H_2 vs time (Figures 11 & 12), three distinct stages (stages I to III in Figures 11 and 12) are observed in these curves:

(1) Region I: the initial period of H_2 gas generation,

(2) Region II: a steady-state reaction region in proceeding reaction with gas film, and

(3) Region III: a degradation period by local deficiency of FeO at the gas-slag interface.

C. Iron species in the reacted and unreacted slags

The different valences of iron in the reacted and un-reacted slags were determined by chemical titration [29]. As shown in **Table 3**, the change in

Fe^{3+} contents between the reacted and un-reacted slags with same basicity increased with increasing the slag basicity from 1.0 to 1.5 and then decreased with further increasing the slag basicity from 1.5 to 2.5, with the maximum value presenting in the slag at basicity of 1.5. With the increasing of FeO concentration from 15% to 30%, the change in Fe^{3+} contents between the reacted and the un-reacted slags with same basicity increased.

D. precipitated phases characterized by XRD

The phases presented in the un-reacted and reacted slags at the continuous cooling rate of 10 K/min were characterized by using XRD and, as an example, **Figure 13** shows the crystallized phases in slag #3.

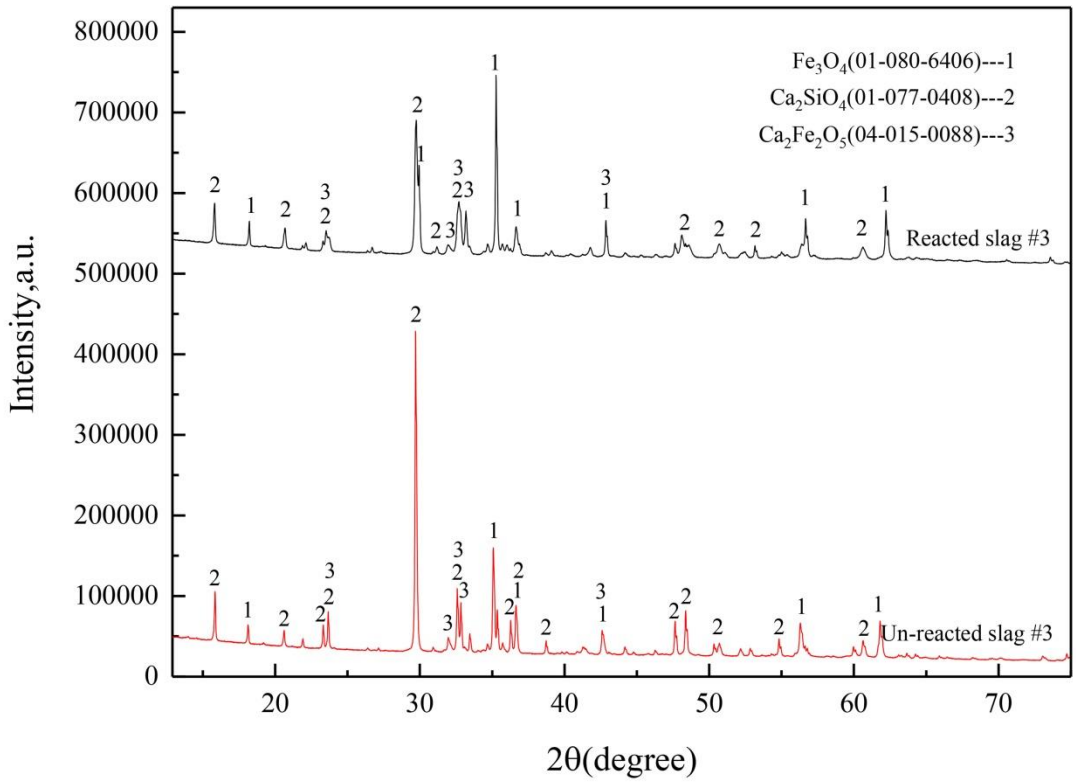

Figure 13 X-ray diffraction patterns of reacted and un-reacted slag #3

Generally, three phases (magnetite Fe_3O_4, Ca_2SiO_4 and $Ca_2Fe_2O_5$) were detected in both the un-reacted and reacted slag #3. However, the main phases in the reacted slag #3 were found to be magnetic spinel (magnetite Fe_3O_4) and di-calcium silicate (Ca_2SiO_4) with a small amount of $Ca_2Fe_2O_5$, while the un-reacted slag comprises mainly di-calcium silicate (Ca_2SiO_4) with a small amount of $Ca_2Fe_2O_5$ and Fe_3O_4. By comparing the integrated intensities of the diffraction peaks from each of the known phases, the weight fraction of magnetic spinel phase in the reacted and un-reacted slags were semi-quantitatively determined and presented in **Table 4**. With the slag basicity increasing from 1.0 to 1.5 to 2.0 to 2.5, the amount of the magnetic spinel phase increases from 4% to 6% (at the basicity of 1.5) and then deceases to 3% to 2% for the un-reacted slags, and increases from 29% to 37% (at the basicity of 1.5) and then deceases to 26% to 22% for the reacted slags. With the increasing of FeO concentration from 15% to 30%, the amount of magnetic spinel phase increases from 1% to 3% for the un-reacted slags and from 18% to 27% for the reacted slags.

IV. DISCUSSION

A. Reaction mechanism and effect of slag composition on H_2 generation

Thermal decomposition of water to produce hydrogen and oxygen can only be achieved thermodynamically at very high temperatures of above 2500 K (2227 °C) and under normal atmospheric pressure. In this study CaO-SiO_2-FeO-MnO-Al_2O_3-MgO slag can be considered as the 'catalyst' or the 'sink' of oxygen which enabled the hydrogen generation from the reaction between CaO-SiO_2-FeO-MnO-Al_2O_3-MgO slags and moisture. Therefore, the reaction between molten CaO-SiO_2-FeO-MnO-Al_2O_3-MgO slag and moisture could be illustrated in **Figure 14.** Consequently,

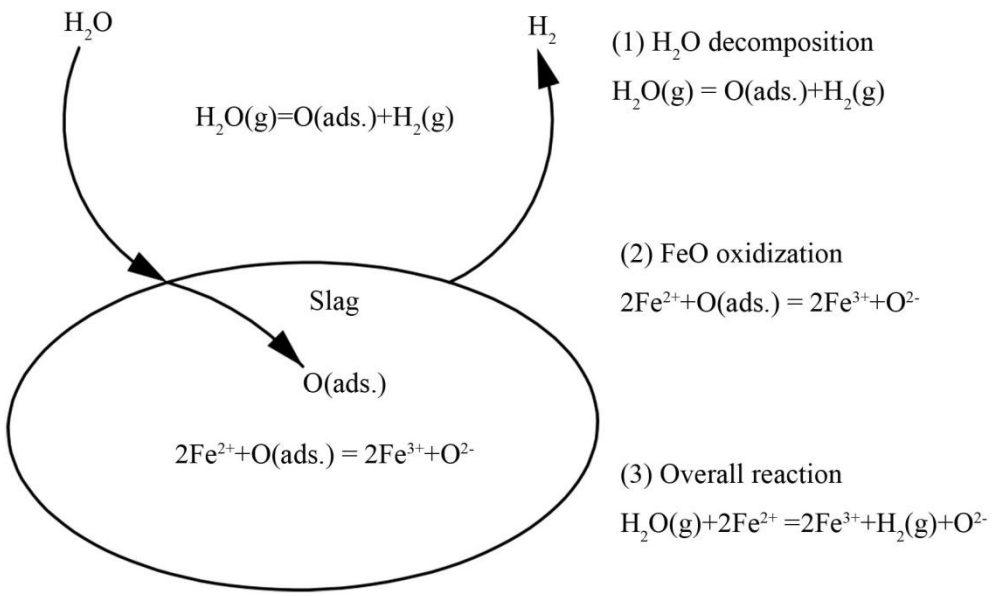

Figure 14 Schematic diagram of the reaction between molten CaO-SiO_2-FeO-MnO-Al_2O_3-MgO slag and moisture

the oxidation of FeO in the molten slag by moisture or the resulting hydrogen generation can be simply considered as the following consecutive two-stage reactions from reaction (1) to reaction (2), and reaction (3) is the overall reaction. The reaction (1) was also suggested by

Glaws and Belton [30] to describe the decomposition of H_2O on the surface of molten iron silicates by using the HDO-H_2 deuterium exchange technique.

$$H_2O(g) = O(ads.)+H_2(g) \quad (1)$$

$$2Fe^{2+}+O(ads.) = 2Fe^{3+}+O^{2-} \quad (2)$$

$$H_2O(g)+2Fe^{2+} = 2Fe^{3+}+H_2(g)+O^{2-} \quad (3)$$

The reaction rate of H_2 generation (reaction (3)) can be calculated by equation (4) by using the off-gas composition.

$$J_{H_2} = \frac{273}{298} \times v_{Ar} \times \frac{V_{H_2}}{22.4 \times V_{Ar}} \bullet \frac{1}{A} \quad (4)$$

where J_{H_2}, A, v_{Ar}, V_{H_2} and V_{Ar} are, the mole flux of H_2 (mol /cm^2/second), the reaction area (cm^2), the flow rate of Ar gas (l/second), the volume fraction of H_2 (%) and the volume fraction of Ar (%) in the off gas composition respectively.

The rate-controlling step(s) for the molten slag – moisture gas reaction in this study can be any or mixed of three steps: 1) gas phase mass transfer, 2) gas-slag reaction, and 3) Fe^{2+} (FeO) diffusion in the liquid slag. The detailed discussion can be found in Appendix. It can be reasonably concluded that under the experimental conditions in this study, the rate-controlling step can be considered as the Fe^{2+} (FeO) diffusion in the liquid slag, which can be particularly the case when the Fe^{2+} (FeO) concentration is decreasing due to its continuous oxidation to

Fe^{3+} (Fe_2O_3). This may explain why the reaction rate is in a linear relationship with the FeO activity in molten slag (Equation (5) and Figure 15).

It is generally believed that with increasing slag basicity the network structure of silicate anion in molten slag is broken by basic component added, [31] resulting in the decrease in strength of the network structure. The change of slag basicity will also change the physicochemical properties such as liquidus temperature and viscosity. In addition to altering the physical properties, the basicity will also alter the activity of FeO. It is therefore reasonable to introduce the activity of FeO instead of the concentration of FeO, since the chemical potential is the driving force of the reaction. [32,33] As shown in **Table 5**, the activity of FeO increases from 0.58 to 0.70 with increasing slag basicity from 1.0 to 2.0, which results in the increase of H_2 gas produced (Reaction (3)). However, with further increasing of the slag basicity to 2.5, the activity of FeO in slag decreases to 0.61, which results in the decrease of H_2 gas produced. With the increasing of slag basicity to 2.5, the slag may contain solid phase, which will increase the viscosity and FeO diffusion rate become small, resulting in the decrease of H_2 gas produced according to reaction (3). A similar trend of FeO activity was reported by Fetters and Chipman, [34] who investigated the equilibria of liquid iron and CaO-MgO-FeO-SiO_2 slags and concluded that activity of FeO reached a distinct local

maximum corresponding to a basicity of approximately 2.0. The similar conclusion was given in the investigation of FeO activities in constituents of iron- and steelmaking slags by Turkdogan. [35] To sum up, the maximum amount of H_2, corresponding to the maximum FeO activity in our study, should be generated for the slag with basicity of 2.0. Similar trend on H_2 generation in the reaction between molten CaO-SiO_2-FeO slag and moisture was also reported by Sato *et al.* [26].

Because alterations of Ar and moist atmosphere in experimental conditions change the reaction rates of regions (I) and (III), the reaction-rate constant is estimated from the slope of region (II), where the concentration of H_2 changes linearly with time (Figures 11 & 12). **Figure 15** shows the relationship between the FeO activity and the measured

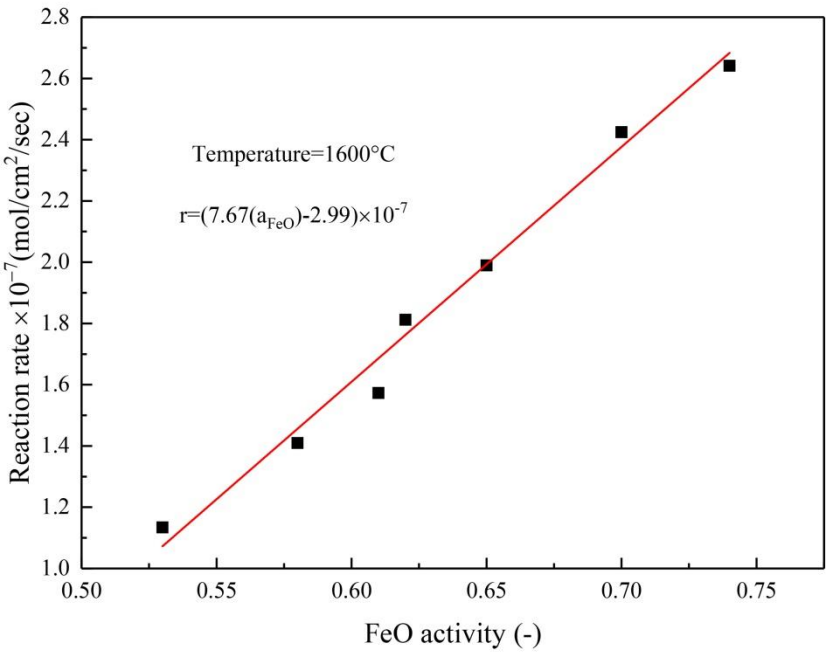

Figure 15 Reaction rate with FeO activity

overall reaction rate, where the activity of FeO in the present slag system was estimated by an interpolation or extrapolation from the known activity of FeO in the CaO-SiO_2-FeO-MgO system at 1873 K (1600 °C) as listed in Table 5. [36, 37] The production rate of H_2 increased with increasing FeO activity at various concentrations of FeO. From the linear relationship of the results, the measured H_2 generation rate (mole/cm^2/second) can be expressed by Eq. (5). A similar relationship between the activity and the reaction rate was reported by Min [38] in spite of the different slag systems and the experimental technique.

$$r = (7.67(a_{FeO}) - 2.99) \times 10^{-7} \quad (5)$$

As shown in **Table 6**, the cumulative H_2 in the reaction between 100 g molten CaO-SiO_2-FeO-MnO-Al_2O_3-MgO slag and moisture was predicted by thermodynamic calculations, measured by using the mass spectrometer, and deducted by chemical titration of Fe^{3+} content in the reacted slag and the un-reacted slag. Both the mass spectrometry and chemical titration data show good agreement except slag #2. However, the data of the accumulated H_2 predicted by thermodynamic calculation is greater than that obtained by both mass spectrometry and chemical titration. While thermodynamic calculation is used for the purpose of predicting the related reactions occurring between molten CaO-SiO_2-FeO-MnO-Al_2O_3-MgO slag and moisture under equilibrium state, the reactions in laboratory experiments are affected by various kinetic factors

such as the reaction time and the reaction area of the slag-gas system. This results in the extent of the studied reactions away from the equilibrium state as predicted by the thermodynamic calculation. As a result, the mass spectrometry, online analyzer, provide more accurate data to evaluate the H_2 generated in the reaction between molten CaO-SiO_2-FeO-MnO-Al_2O_3-MgO slag and moisture at 1873 K (1600 °C).

B. Comparison of magnetic spinel phase determined by different methods

As shown in **Table 7**, the amount of magnetic spinel phase in the studied slags was predicted by thermodynamic calculations and semi-quantitatively determined by XRD. Both the thermodynamic calculation and XRD data show similar trend. However, the amount of magnetic spinel phase predicted by thermodynamic calculation is less than that determined by XRD. This is because the number of the phases presented in the laboratory slags (three phases in Figure 13) is much less than that predicted by FactSage 7.0 in equilibrium condition (six phases for un-reacted slag in Figure 4 and seven phases for the reacted slag in Figure 5), which results in the relative high amount of the phases determined by XRD. It is seen that, with increasing slag basicity, the maximum amount of magnetic spinel phase was generated in the slag with basicity of 1.5. However, previous discussion on the H_2 generation indicated that, the maximum amount of the H_2 was generated in the slag

with basicity of 2.0. The difference between the maximum amount of H_2 and magnetic spinel phase should be attributed to the generation of calcium ferrite ($Ca_2Fe_2O_5$) by the reaction (6) [39] with the increasing of slag basicity. As shown in Table 2, when the slag basicity is small than 2.0, the generated Fe_2O_3 by the reaction (3) is mainly forming Fe_3O_4 by the reaction of $Fe_2O_{3(s)} + FeO_{(l)} = Fe_3O_{4(s)}$ and the maximum amount of magnetic spinel phase was generated in the slag with basicity of 1.5. However, when the slag basicity is equal to or above 2.0, the reaction (6) occurred, resulting in the decreasing of transformation of Fe_2O_3 into Fe_3O_4.

$$2CaO + 2FeO + H_2O = H_2 + Ca_2Fe_2O_5 \quad (6)$$

For the slags with basicity of 2.0, the amount of both magnetic spinel and $Ca_2Fe_2O_5$ increase with the increasing of FeO concentration from 15% to 30%. In general, FeO in the silicate slag, plays a same role as CaO to break the network structure of silicate anion in molten slag, resulting in decreasing of the viscosity, softening and melting temperatures of the slag systems, closely correspond to the changes in FeO activity in molten slag. **Figure 16** shows the comparison of the variation of FeO activity

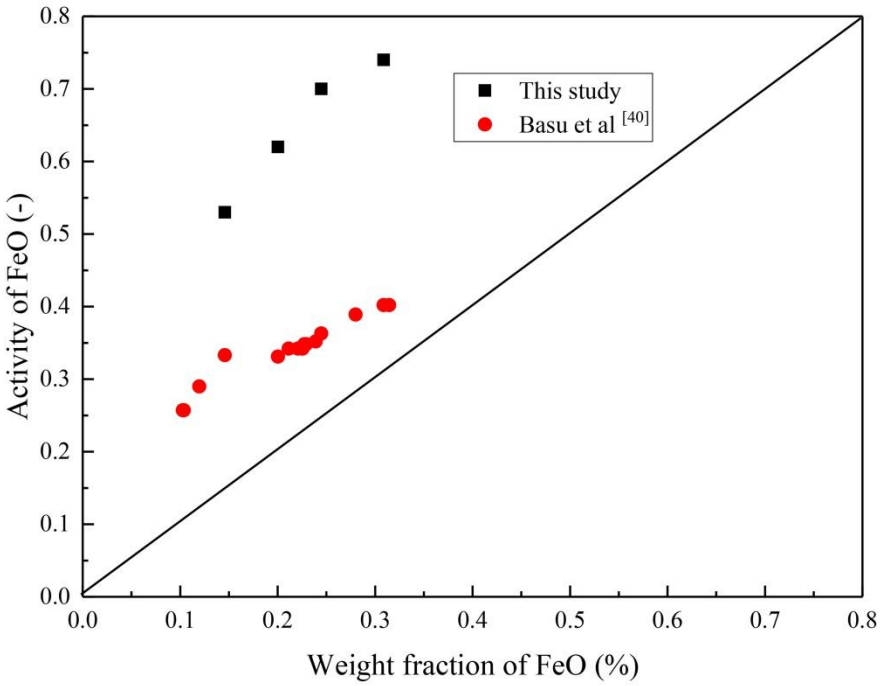

Figure 16 Comparison of variation of FeO activity with FeO concentration at 1873 K (1600 °C) for slags with basicity of 2.0 between Basu[40] and this study

with FeO concentration at the basicity of 2.0 between Basu *et al.* [40] and this study. It should be noted that the slags with the basicity of approximately 2 (from 1.9 to 2.1) from Basu's work was selected to plot the Figure 16. The figure shows a nearly linear increase of the FeO activity with increasing FeO concentration, and clearly illustrates that the activity of FeO exhibits positive deviation. A similar trend was reported by Kishimoto et al.[41] and by Bodsworth.[42] As a result, in the present study, the amount of Fe^{3+} containing phases (magnetic spinel phase and $Ca_2Fe_2O_5$) increased since the FeO activity in molten CaO-SiO_2-FeO-MnO-Al_2O_3-MgO slag at 1873 K (1600 °C) increased with increasing the

FeO concentration from 15% to 30%.

The presence of Fe^{3+} containing phases including magnetic spinel and calcium ferrite ($Ca_2Fe_2O_5$) in the un-reacted slags, as analyzed by chemical titration in Table 3 and determined by XRD in Figure 13, should be attributed to the oxygen partial pressure in the Ar gas, which results in the partly oxidization of FeO at the high temperature. Based on the composition of gases in Figure 9, the oxygen partial pressure in the Ar atmosphere in this study is 2.62×10^{-5} Pa, corresponding to the dot line marked in **Figure 17**, and the magnetic spinel phase, mainly made up of

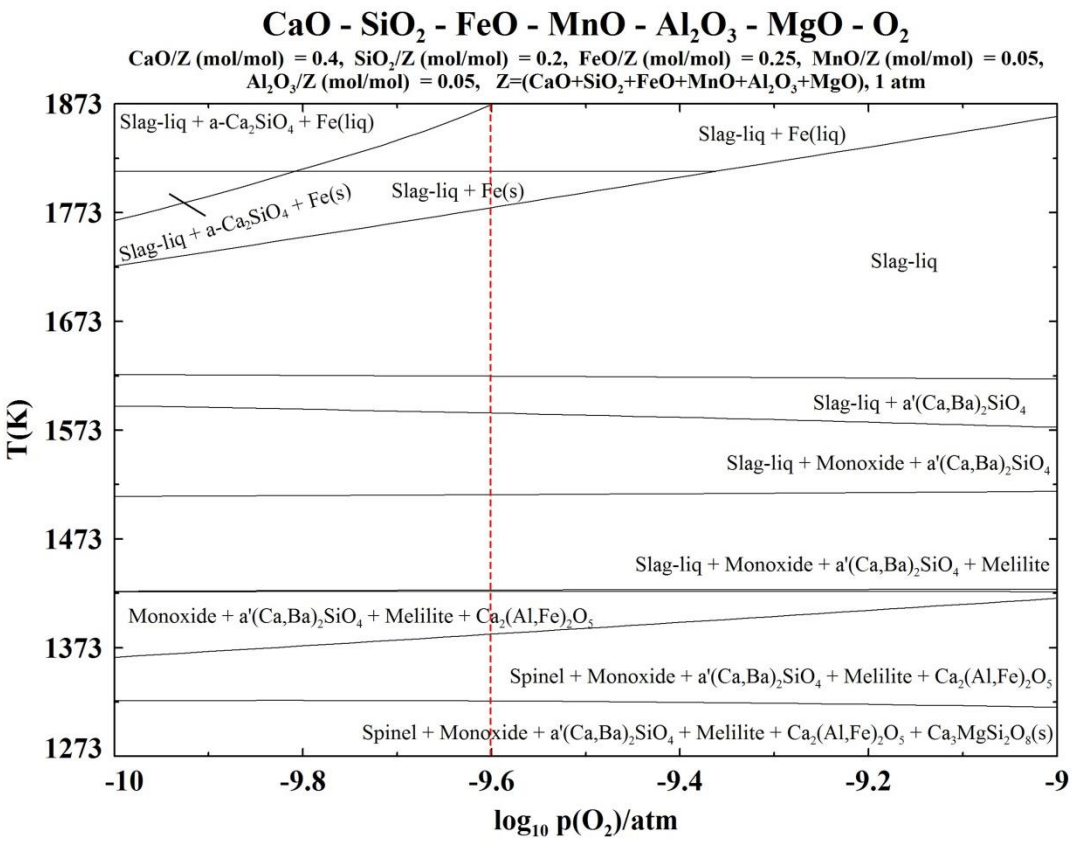

Figure 17 Precipitated phases of CaO-SiO_2-FeO-MnO-Al_2O_3-MgO slag with oxygen partial pressure

magnetite Fe_3O_4, thermodynamically starts to precipitate from the liquid

slag when the temperature is lower than 1197℃.

V. CONCLUSIONS

A novel process for energy (in the form of fuel gas) and materials (in the form of magnetite Fe_3O_4) recovery in steelmaking slags has been investigated by both thermodynamic calculation and laboratory experiments. This process is based on the reaction of molten steelmaking slag with the moist atmosphere. The capability of this process was fundamentally verified by online measuring H_2 production, determining the conversion from Fe^{2+} to Fe^{3+} via titration analysis and quantifying the magnetite Fe_3O_4 amount for the slags with different basicities and FeO concentrations. The results are stated below.

The thermodynamic calculation showed that, for 100 g slags reacting with 100 g H_2O, with increasing slag basicity (CaO/SiO_2) from 1.0 to 2.5, the accumulated amount of produced H_2 gas increased from 0.17 g to 0.27 g, and the amount of magnetic spinel phase first increased and then decreased, with the maximum of 16.71 g presenting in the slags with basicity of 1.5. With increasing the FeO concentration from 15% to 30%, the accumulated amount of produced H_2 increased from 0.17 g to 0.28 g, while the amount of magnetic spinel phase increased from 5.88 g to 10.59 g.

The laboratory experiments were conducted in confocal laser scanning microscope to verify the reaction between 0.2 g slag and 3.75 l H_2O-Ar gas ($P_{H_2O} = 0.2atm$). The results indicated that, for 100 g slags, with increasing slag basicity (CaO/SiO_2) from 1.0 to 2.5, both the produced H_2 gas and magnetic spinel phase first increased and then decreased, with the maximum of 0.09 g and 37.00 g presenting in the slag with basicity of 1.5. In the case of FeO concentration increasing from 15% to 30%, both the produced H_2 gas and the magnetic spinel phase increased from 0.04 g to 0.10 g and from 18.00 g to 27.00 g respectively.

The rate of hydrogen generation from the reaction between molten CaO-SiO_2-FeO-MnO-Al_2O_3-MgO slag and the moisture ($P_{H_2O} = 0.2atm$) increased with increasing FeO activity in the slag. Its dependence on FeO content can be expressed as $r = (7.67(a_{FeO}) - 2.99) \times 10^{-7}$ (mol/cm^2/sec).

Acknowledgements

This work was supported by Innovate UK (for Tata Steel UK), EPSRC (for University of Warwick EP/M507829/1), and MOST (Ministry of Science and Technology) China (for USTB and Shougang Corp.) under the project No. 102170. The author Zushu Li would like to thank EPSRC for financial support under grant number EP/N011368/1.

References

[1] H. Motz and J. Geiseler: *Waste Manage.*, 2001, vol. 21, pp. 285-93.

[2] H. Yi, G. Xu, H. Cheng, J. Wang, Y. Wan and H. Chen: *Procedia Environmental Sciences*, 2012, vol. 16, pp. 791-801.

[3] E. Kasai, T. Kitajima, T. Akiyama, J.I. Yagi and F. Saito: *ISIJ Int.*, 1997, vol. 37, pp. 1031-36.

[4] M.L. Andrade, L. Almeida, M. Rangel, F. Pompeo and N. Nichio: *Chem. Eng. Technol.*, 2014, vol. 37, pp. 343-48.

[5] A.W. Bhutto, A.A. Bazmi and G. Zahedi: *Prog. Energy Combust. Sci.*, 2013, vol. 39, pp. 189-214.

[6] S. Shabbar and I. Janajreh: *Energy Convers. Manag.*, 2013, vol. 65, pp. 755-63.

[7] A.V. Bridgwater: *Fuel*, 1995, vol. 74, pp. 631-53.

[8] S. Luo, C. Yi and Y. Zhou: *Renew Energy*, 2013, vol. 50, pp. 373-77.

[9] V. Hacker, R. Fankhauser, G. Faleschini, H. Fuchs, K. Friedrich, M. Muhr and K. Kordesch: *J. Power Sources*, 2000, vol. 86, pp. 531-35.

[10] B. Malvoisin, F. Brunet, J. Carlut, G.M. Hernandez, N. Findling, M. Lanson, O. Vidal, J.Y. Bottero and G. Bruno: *Int. J. Hydrog. Energy*, 2013, vol. 38, pp. 7382-93.

[11] J. Nakano and J. Bennett: *Int. J. Hydrog. Energy*, 2014, vol. 39, pp. 4954-58.

[12] K. Nishioka, T. Maeda and M. Shimizu: *ISIJ Int.*, 2006, vol. 46, pp. 427-33.

[13] Y. Kang and K. Morita: *ISIJ Int.*, 2006, vol. 46, pp. 420-26.

[14] H.G. Ryu, Z.T. Zhang, J.W. Cho, G.H. Wen and S. Sridhar: *ISIJ Int.*, 2010, vol. 50, pp. 1142-50.

[15] Y.Q. Sun, H.W. Shen, H. Wang, X.D. Wang and Z.T. Zhang: *Energy*, 2014, vol. 76, pp. 761-67.

[16] T. Nomura, N. Okinaka and T. Akiyama: *ISIJ Int.*, 2010, vol. 50, pp. 1229-39.

[17] Y.Q. Sun, Z.T. Zhang, L.L. Liu and X.D. Wang: *Energies*, 2014, vol. 7, pp. 1673-84.

[18] J. Li, D. Bhattacharjee, X. Hu, D. Zhang, S. Sridhar and Z. Li: *Mineral Processing and Extractive Metallurgy*, 2017, vol. 126, pp. 94-105.

[19] K. Morita, M. Guo, N. Oka and N. Sano: *Journal of Material Cycles and Waste Management*, 2002, vol. 4, pp. 93-101.

[20] S.L. Teasdale and P.C. Hayes: *ISIJ Int.*, 2005, vol. 45, pp. 642-50.

[21] B. Bhoi, A.K. Jouhari, H.S. Ray and V.N. Misra: *Ironmaking & Steelmaking*, 2006, vol. 33, pp. 245-52.

[22] A. Semykina, J. Nakano, S. Sridhar, V. Shatokha and S. Seetharaman: *Metall. Mater. Trans. B*, 2011, vol. 42B, pp. 471-76.

[23] A. Semykina, J. Nakano, S. Sridhar, V. Shatokha and S. Seetharaman: *Metall. Mater. Trans. B*, 2010, vol. 41B, pp. 940-45.

[24] A. Semykina: *Metall. Mater. Trans. B*, 2012, vol. 43B, pp. 56-63.

[25] D. Bhattacharjee, T. Mukharjee and V. Tathavadkar: 2007. Set-up for production of hydrogen gas by thermos-chemical decomposition of water using steel plant slag and waste materials, Tata Steel Limited, Publication No.: WO2007125537 A1.

[26] T. Mukherjee and D. Bhattacharjee: 2007. A method for producing hydrogen and/or other gases from steel plant wastes and waste heat, Tata Steel Limited, Publication No.: WO2007036953 A1.

[27] H. Matsuura and F. Tsukihashi: *ISIJ Int.*, 2012, vol. 52, pp. 1503-12.

[28] M. Sato, H. Matsuura and F. Tsukihashi: *ISIJ Int.*, 2012, vol. 52, pp. 1500-02.

[29] B.R. Sant and T.P. Prasad: *Talanta*, 1968, vol. 15, pp. 1483-86.

[30] P.C. Glaws and G.R. Belton: *Metal. Trans. B*, 1990, vol. 21B, pp. 511-19.

[31] R.G. Ward: An Introduction to the Physical Chemistry of Iron & Steel Making, Edward Arnold LTD, London, 1962, pp. 9.

[32] M. Sugata, T. Sugivama and S. Kondo: *Tetsu-to-Hagané*, 1972, vol. 10, pp. 11-23.

[33] S. Hara and K. Ogini: *Tetsu-to-Hagané*, 1990, vol. 76, pp. 54-61.

[34] K.L. Fetters and J. Chipman: *Trans. AIME*, 1941, vol. 145, pp. 95-112.

[35] E.T. Turkdogan and J. Pearson: *J. Iron Steel Inst.*, 1953, vol. 173, pp. 217-23.

[36] C.R. Taylor and J. Chipman: *Trans. AIME*, 1943, vol. 154, pp. 228-47.

[37] V.D. Eisenhuttenleute: *Slag Atlas.*, 2nd ed., Verlag Stahleisen GmbH, Dusseldorf/Germany, 1995, pp. 254.

[38] D.J. Min, J.W. Han and W.S. Chung: *Metall. Mater. Trans. B*, 1999, vol. 30, pp. 215-21.

[39] V. Shatokha, I. Sokur and L. Kamkina: *J. Sustain. Metall.*, 2016, vol. 2, pp. 116-22.

[40] S. Basu, A.K. Lahiri and S. Seetharaman: *Metall. Mater. Trans. B*, 2008, vol. 39, pp. 447-56.

[41] T. Kishimoto, M. Hasegawa, K. Ohnuki, T. Sawai, and M. Iwase:

Steel Res. Int., 2005, vol. 76, pp. 341- 47.

[42] C. Bodsworth: *J. Iron Steel Inst.*, 1959, vol. 193, pp. 13-24.

[43] S. Taniguchi, A, Kikuchi and S. Maeda: *Tetsu-to-Hagane*, 1977, vol. 63, pp.1071-80.

[44] E. Kasai, T, Kitajima, T. Akiyama, J. Yagi and F. Saito: *ISIJ Int.*, 1997, vol. 37, pp.1031-36.

[45] J.R. Welty, C.E. Wicks, R.E. Wilson and G. Rorrer: *Fundamentals of Momentum, Heat and Mass Transfer*, 5th ed., John Wiley & Sons, New York, NY, 2007, pp.686.

[46] P. Křenek: *Plasma Chemistry and Plasma Processing*. 2008, vol. 28, pp. 107-122.

[47] S. Ranjan, S. Sridhar and R.J. Fruehan: *Energy & Fuels*, 2010, vol. 24, pp.5002–5007.

Table captions:

Table 1 Chemical composition of synthesized slag samples (wt.%)

Table 2 The amount of the Fe^{3+} containing phases (g) in the reacted slags

Table 3 Different valences of iron in the reacted and un-reacted slags determined by chemical titration

Table 4 Weight fraction (%) of spinel phase in the un-reacted and reacted slags at the continuous cooling rate of 10 K/min

Table 5 Activity of FeO in CaO-SiO_2-FeO-MgO slag at 1873 K (1600 °C) [36, 37]

Table 6 The amount of the accumulated H_2 obtained by thermodynamic calculation, mass spectrometry and chemical titration (g)

Table 7 Comparison of spinel amount obtained by thermodynamic calculation and XRD (g)

Table 1 Chemical composition of synthesized slag samples (wt.%)

Samples	CaO	SiO_2	FeO	Al_2O_3	MgO	MnO	CaO/SiO_2
#1	29.49	29.93	25.88	4.83	4.93	4.93	0.99
#2	35.67	24.11	25.68	4.89	4.85	4.81	1.48
#3	39.38	19.94	26.12	4.85	4.89	4.82	1.97
#4	42.01	17.06	26.30	4.93	4.82	4.89	2.46
#5	46.11	23.07	15.96	4.91	4.97	4.98	2.00
#6	42.76	21.47	20.98	4.88	4.97	4.93	1.99
#7	36.04	18.17	31.21	4.92	4.85	4.82	1.98

Table 2 The amount of the Fe^{3+} containing phases (g) in the reacted slags

Samples	#1	#2	#3	#4	#5	#6	#7
Spinel	13.99	16.71	10.03	7.39	5.88	9.46	10.59
$Ca_2(Al,Fe)_2O_5$	0	0	14.61	27.01	12.06	13.07	15.64

Table 3 Different valences of iron in the reacted and un-reacted slags determined by chemical titration

	Fe^{2+}/%	TFe/%	Fe^{3+}/%	ΔFe^{3+}(Fe^{3+}(R)- Fe^{3+}(U))/%
1# (U)	14.9	26.2	11.3	
1# (R)	11.6	26.2	14.6	3.3
2# (U)	12.6	25.7	13.1	
2# (R)	6.5	25.7	19.2	6.1
3# (U)	12.8	23.9	11.1	
3# (R)	7.4	23.9	16.5	5.4
4# (U)	14.4	21.5	7.1	
4# (R)	10.7	21.5	10.8	3.7
5# (U)	9.6	15.8	6.2	
5# (R)	7.0	15.8	8.8	2.6
6# (U)	12.9	19.5	6.6	
6# (R)	8.8	19.5	10.7	4.1
7# (U)	17.1	28.4	11.3	
7# (R)	9.8	28.4	18.6	7.3

U indicates the un-reacted slags, R indicates the reacted slags.

Table 4 Weight fraction (%) of spinel phase in the un-reacted and reacted slags at the continuous cooling rate of 10 K/min

Slag	#1	#2	#3	#4	#5	#6	#7
Un-reacted	4	6	3	2	1	2	3
Reacted	29	37	26	22	18	24	27

Table 5 Activity of FeO in $CaO-SiO_2-FeO-MgO$ slag at 1873 K (1600 °C) [36, 37]

#1	#2	#3	#4	#5	#6	#7
0.58	0.65	0.70	0.61	0.53	0.62	0.74

Table 6 Comparison of accumulated H_2 amount obtained by thermodynamic calculation, mass spectrometry and chemical titration (g)

	#1	#2	#3	#4	#5	#6	#7
Thermodynamic calculation	0.17	0.22	0.25	0.27	0.17	0.21	0.28
Mass spectrometry	0.05	0.08	0.09	0.06	0.04	0.07	0.10
Chemical titration	0.06	0.11	0.10	0.07	0.05	0.07	0.13

Table 7 Comparison of spinel amount obtained by thermodynamic calculation and XRD (g)

	#1	#2	#3	#4	#5	#6	#7
Thermodynamic calculations	13.99	16.71	10.03	7.39	5.88	9.46	10.59
XRD	29	37	26	22	18	24	27

Figure captions:

Figure 1 Schematic diagram of experimental apparatus: 1. Retort stand; 2. Round-bottom flask; 3. Heating mantles; 2. Temperature probe; 5. Heater tape; 6. Halogen lamp; 7.Thermocouple; 8. Temperature controller; 9. Samples; 10. Platinum crucible; 11. Furnace chamber; 12. Lens; 13. Beam splitter; 14. He-Ne laser; 15. Pin hole; 16. Ion source; 17. Accelerating voltage; 18. Electromagnet; 19. Vacuum pump; 20. Detector

Figure 2 Change in the accumulated amount of H_2 gas produced as a function of the mass of H_2O introduced at different slag basicities

Figure 3 Change in the accumulated amount of H_2 gas produced as a function of the mass of H_2O introduced at different FeO concentrations

Figure 4 Change in the total amount of different phases precipitated from un-reacted slag #3

Figure 5 Change in the total amount of different phases precipitated from reacted slag #3

Figure 6 Constituents of spinel phase generated in the reacted slag #3

Figure 7 Change in the accumulated amount of spinel phase precipitated from reacted slags with different basicities

Figure 8 Change in the accumulated amount of spinel phase precipitated from reacted slags with different FeO concentrations

Figure 9 Gas composition for the unreacted slag as determined by mass spectrometry

Figure 10 Gas composition for the reacted slag (slag 3#) as determined by mass spectrometry

Figure 11 Changes of accumulated H_2 as a function of reaction time for slags with different basicities

Figure 12 Changes of accumulated H_2 as a function of reaction time for slags with different FeO concentrations

Figure 13 X-ray diffraction patterns of reacted and un-reacted slag #3

Figure 14 Schematic diagram of the reaction between molten CaO-SiO_2-FeO-MnO-Al_2O_3-MgO slag and moisture

Figure 15 Reaction rate with FeO activity

Figure 16 Comparison of variation of FeO activity with FeO concentration at 1873 K (1600 °C) for slags with basicity of 2.0 between Basu [40] and this study

Figure 17 Precipitated phases of CaO-SiO_2-FeO-MnO-Al_2O_3-MgO slag with oxygen partial pressure

Appendix

In general, the rate-controlling step(s) for the molten slag – moisture gas reaction in this study can be any or mixed of three steps: 1) gas phase mass transfer, 2) gas-slag reaction, and 3) Fe^{2+} (FeO) diffusion in the liquid slag. Under the experimental conditions in this study, the rate-controlling step can be considered as the Fe^{2+} (FeO) diffusion in the liquid slag, which can be particularly the case when the Fe^{2+} (FeO) concentration is decreasing due to its continuous oxidation to Fe^{3+} (Fe_2O_3). This is because the diffusion of FeO in liquid slag is found to be the lowest among the three steps.

1) Gas phase transport of reactants

According to Taniguchi et al [43] and Kasai et al [44], an empirical equation of the mass transfer rate N (mol/(s·m^2)) to the vertical direction in the gas phase for an experimental set-up similar to the present case is given by equation (A1):

$$N = k_g \Delta P / \left(R T_g \right) \tag{A1}$$

where ΔP is the partial pressure difference of transferring gas between gas film and bulk stream and k_g is the mass transfer coefficient (m/s) calculated by equations (A2) and (A3) [45]:

$$Sh_x = 0.332 \cdot (\mathrm{Re})^{\frac{1}{2}} \cdot (Sc)^{\frac{1}{3}} \tag{A2}$$

$$Sh_x = \frac{K_g L}{D_g} \tag{A3}$$

$$K_g = \frac{D_g}{L} \cdot Sh_x = \frac{D_g}{L} \cdot 0.332 \cdot (\mathrm{Re})^{\frac{1}{2}} \cdot (Sc)^{\frac{1}{3}} = \frac{D_g}{L} \cdot 0.332 \cdot (\frac{u_g \cdot \mathrm{R}}{\nu})^{\frac{1}{2}} \cdot (\frac{\nu}{D_g})^{\frac{1}{3}}$$
$$= 0.332 \cdot D_g^{\frac{2}{3}} \cdot (\mathrm{R})^{-\frac{1}{2}} \cdot (\nu)^{-\frac{1}{6}} \cdot (u_g)^{\frac{1}{2}}$$

where D_g: diffusion coefficient of gas (m^2/s), R: radius of the crucibles (m), ν: kinematic viscosity (m^2/s), u_g: linear velocity of gas (m/s). $\nu = 2.17 \times 10^{-5}$ m^2/s [45], D_g was estimated from the values of a literature assuming a Ar-H_2O system which is the main component of the gas mixture in the present work, with the value of 8×10^{-5} m^2/s [46], R=0.0045 m，$u_g = 5.0 \times 10^{-6} m^3/s$

$$K_g = 0.332 \cdot (8 \times 10^{-5})^{\frac{2}{3}} \cdot (0.0045)^{-\frac{1}{2}} \cdot (2.17 \times 10^{-5})^{-\frac{1}{6}} \cdot (5 \times 10^{-6})^{\frac{1}{2}}$$
$$= 0.332 \times 1.86 \times 10^{-3} \times 14.91 \times 5.99 \times 2.24 \times 10^{-3}$$
$$= 1.24 \times 10^{-4} m/s$$

As a result,

$$N = k_g \Delta P / \left(RT_g\right) = 1.24 \times 10^{-4} \times 0.2 \times 1.01 \times 10^5 / (8.31 \times 373) = 7.87 \times 10^{-3} mol/(m^2 s)$$

2) Gas-slag reaction at the gas-slag interface

Based on the investigation results of Glaws and Belton [30], the rate of dissociation of H_2O on silica-saturated iron silicate melts can be expressed in the equation (A4)

$$v = k p_{H_2O} (Fe^{3+} / Fe^{2+})^{-2} \quad \text{(A4)}$$

where k is a temperature-dependent constant, in units of mol/(cm^2s), can be given by the approximate expression $\log k$=-6700/T-0.08.

As a result, for the temperature 1873K and $P_{H_2O} = 0.2atm$, k = 0.000044 mol/(cm^{2}s) = 0.44 mol/(m^{2}s).

3) Diffusion of FeO in liquid slag

According to the investigation regarding the rate and rate-controlling reaction of FeS droplets with simplified reactor gas and slags determined using a confocal scanning laser microscope (CSLM)[47], the mass transfer of FeO in the liquid slag phase could be given by equation (A5).

$$J_{FeO} = \frac{m_s \rho_s}{100 M_{FeO}} [(\%FeO)_B - (\%FeO)_E] \quad \text{(A5)}$$

Where, m_s is the mass transfer coefficient in the slag, $(\%FeO)_B$, $(\%FeO)_E$ are the bulk and equilibrium FeO content, respectively, and M_{FeO} is the molecular weight of FeO.

$$\mathrm{H_2}(g) + \frac{1}{2}\mathrm{O_2}(g) = \mathrm{H_2O}(g)$$

$$\Delta G^{\theta} = -251880 + 58.33T \quad \text{(T=1500-2000K)}$$

$$P_{O_2} = (\frac{P_{H_2O}}{P_{H_2}})^2 \cdot \frac{1}{(K^{\theta})^2}$$

$$\lg P_{O_2} = 2\lg(\frac{P_{H_2O}}{P_{H_2}}) - 2\lg K^{\theta}$$

When T=1873K,

$$\lg K^{\theta} = = \frac{251880}{19.147 \times 1873} - \frac{58.33}{19.147} = 6.93 - 3.05 = 3.88$$

As illustrated in Table 6, the accumulated H_2 amount of slag #3 obtained by mass spectrometry was 0.09g (1.04 l) for 10 minutes, while about 1875 l H_2O-Ar gas ($P_{H_2O} = 0.2atm$) was introduced into CLSM during the reaction, which was equal to the total volume of steam 375 l for 10 minutes. As a result, the $\frac{P_{H_2O}}{P_{H_2}}$ can be simply considered 360.58 as the uncertainty in the shape and exposed area makes a detailed analysis of the onsite gas composition difficult.

$$\lg P_{O_2} = 2\lg(\frac{P_{H_2O}}{P_{H_2}}) - 2\lg K^{\theta} = 2\times\lg 360.58 - 2\times 3.88 = 5.11 - 7.76 = -2.65$$

$$P_{O_2} = 2.24\times10^{-3}\text{atm, or } P_{O_2} = 224\text{Pa}$$

Based on the equation (2) in the section "A. Reaction mechanism and effect of slag composition on H_2 generation" and the oxygen partial pressure of 224Pa, for an initial FeO content ranging from 15% to 30% in 100 mg slag, there will be no Fe^{2+} in the final slag if all Fe^{2+} reacts to Fe^{3+}. As a result, $(\%FeO)_E$ can be considered to be 0 when the reaction reaches equilibrium. Taking slag #3 as an example (25% FeO), then the mass transfer of FeO in slag can be calculated as:

$$J_{FeO} = \frac{0.004\times3}{100\times72}\times25 = 4.17\times10^{-3} \quad \text{mol/(m}^2\text{s)}$$

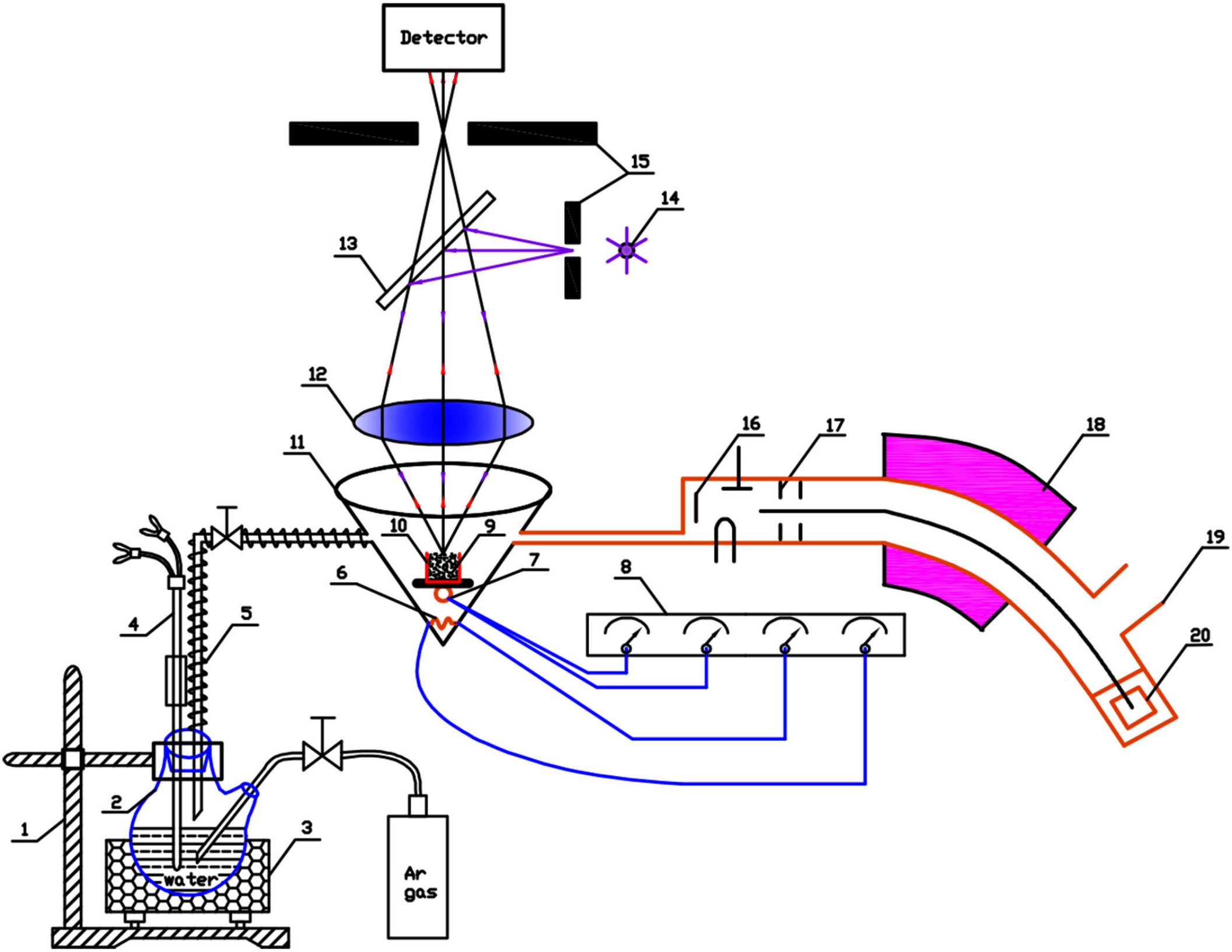
Detector
15
14
13
12
11
16
17
18
10
9
7
6
8
19
20
4
5
2
1
3
water
Ar
gas

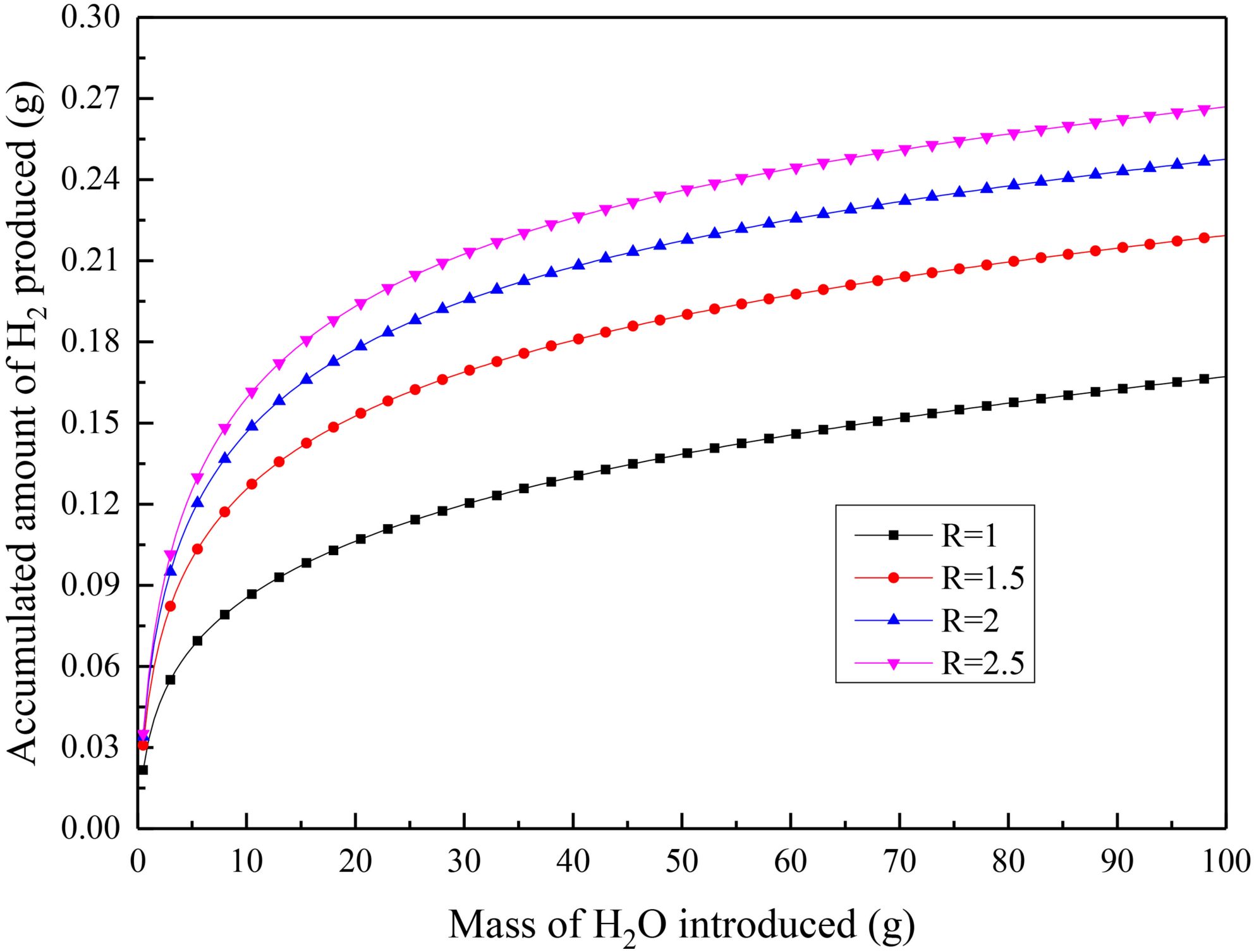
0.30
0.27
0.24
0.21
0.18
0.15
0.12
0.09
0.06
0.03
0.00
Accumulated amount of H_2 produced (g)
0
10
20
30
40
50
60
70
80
90
100
Mass of H_2O introduced (g)
R=1
R=1.5
R=2
R=2.5

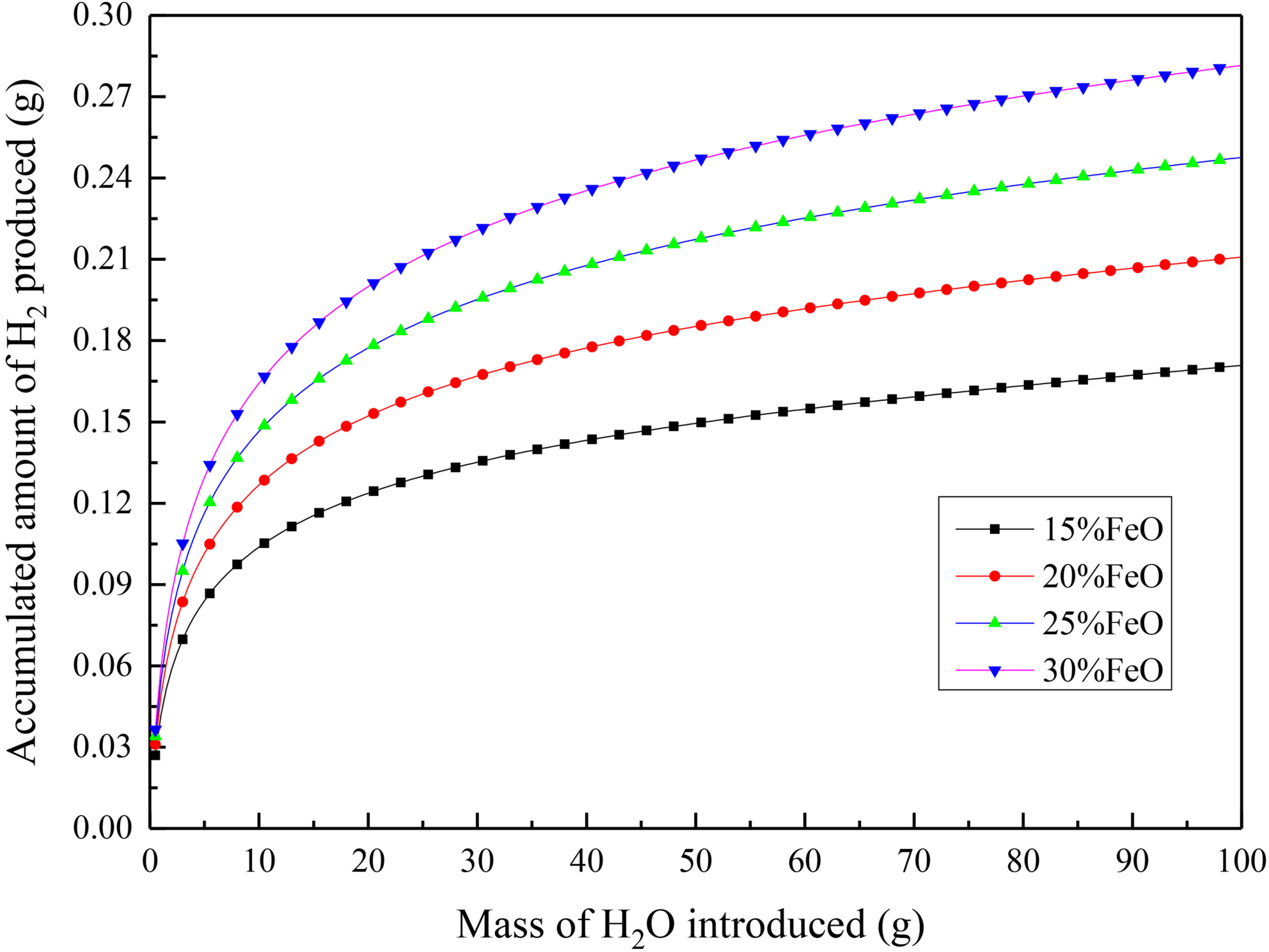
0.30
0.27
0.24
0.21
0.18
0.15
0.12
0.09
0.06
0.03
0.00
Accumulated amount of H_2 produced (g)
0
10
20
30
40
50
60
70
80
90
100
Mass of H_2O introduced (g)
15%FeO
20%FeO
25%FeO
30%FeO

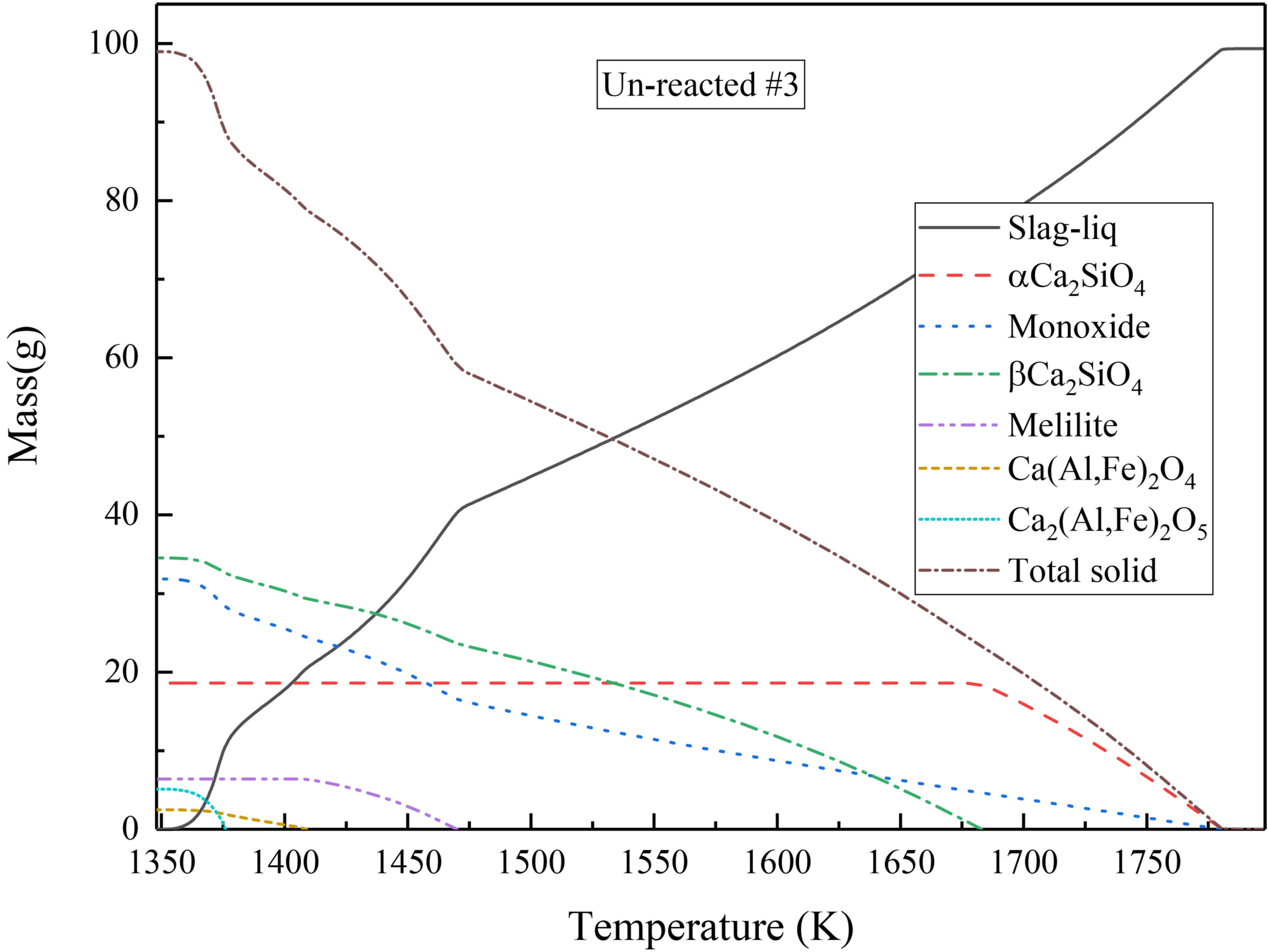
Un-reacted #3
Slag-liq
αCa2SiO4
Monoxide
βCa2SiO4
Melilite
Ca(Al,Fe)2O4
Ca2(Al,Fe)2O5
Total solid
Mass(g)
Temperature (K)
0
20
40
60
80
100
1350
1400
1450
1500
1550
1600
1650
1700
1750

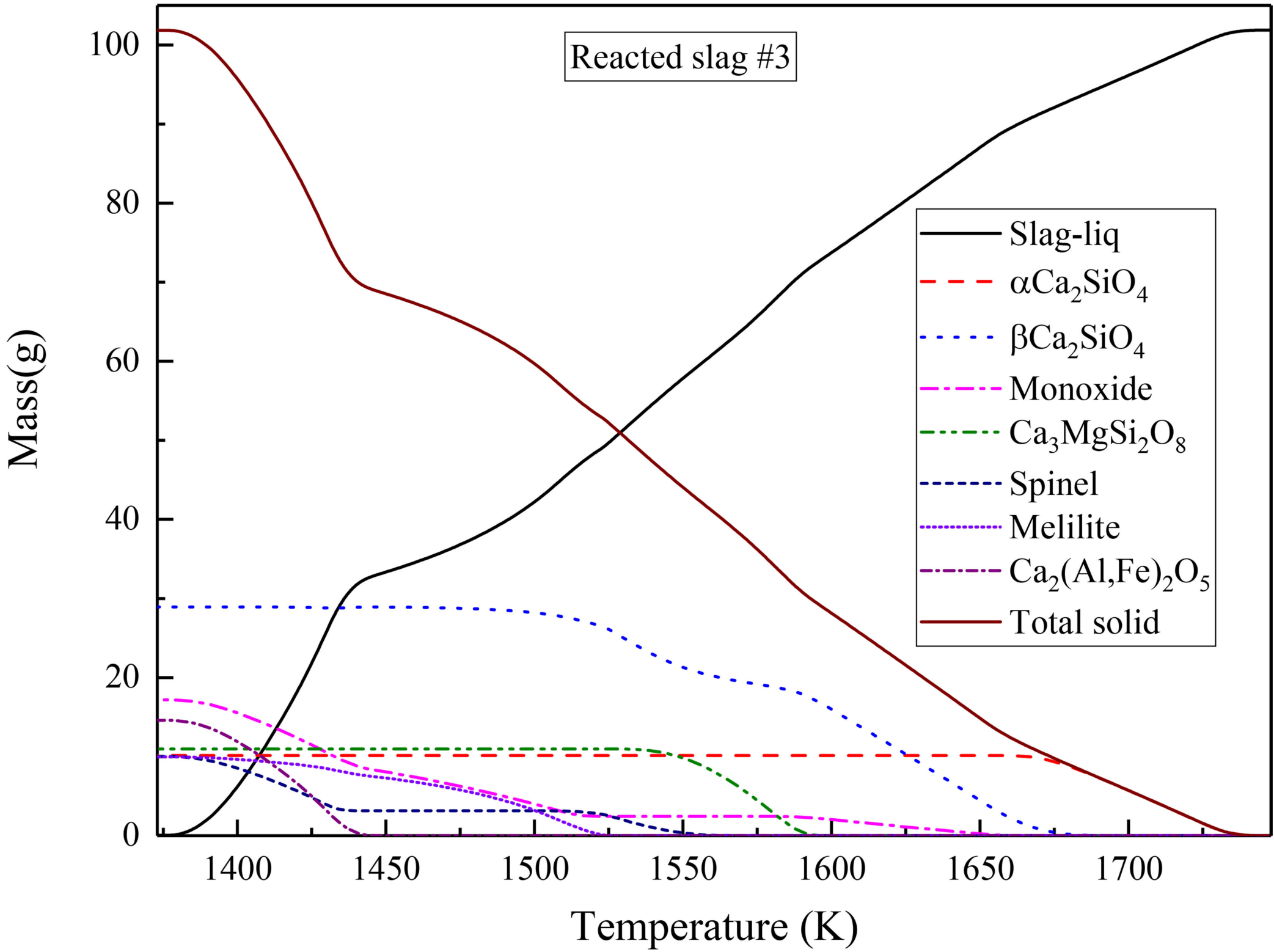
Reacted slag #3
Mass(g)
Temperature (K)
0
20
40
60
80
100
1400
1450
1500
1550
1600
1650
1700
Slag-liq
αCa2SiO4
βCa2SiO4
Monoxide
Ca3MgSi2O8
Spinel
Melilite
Ca2(Al,Fe)2O5
Total solid

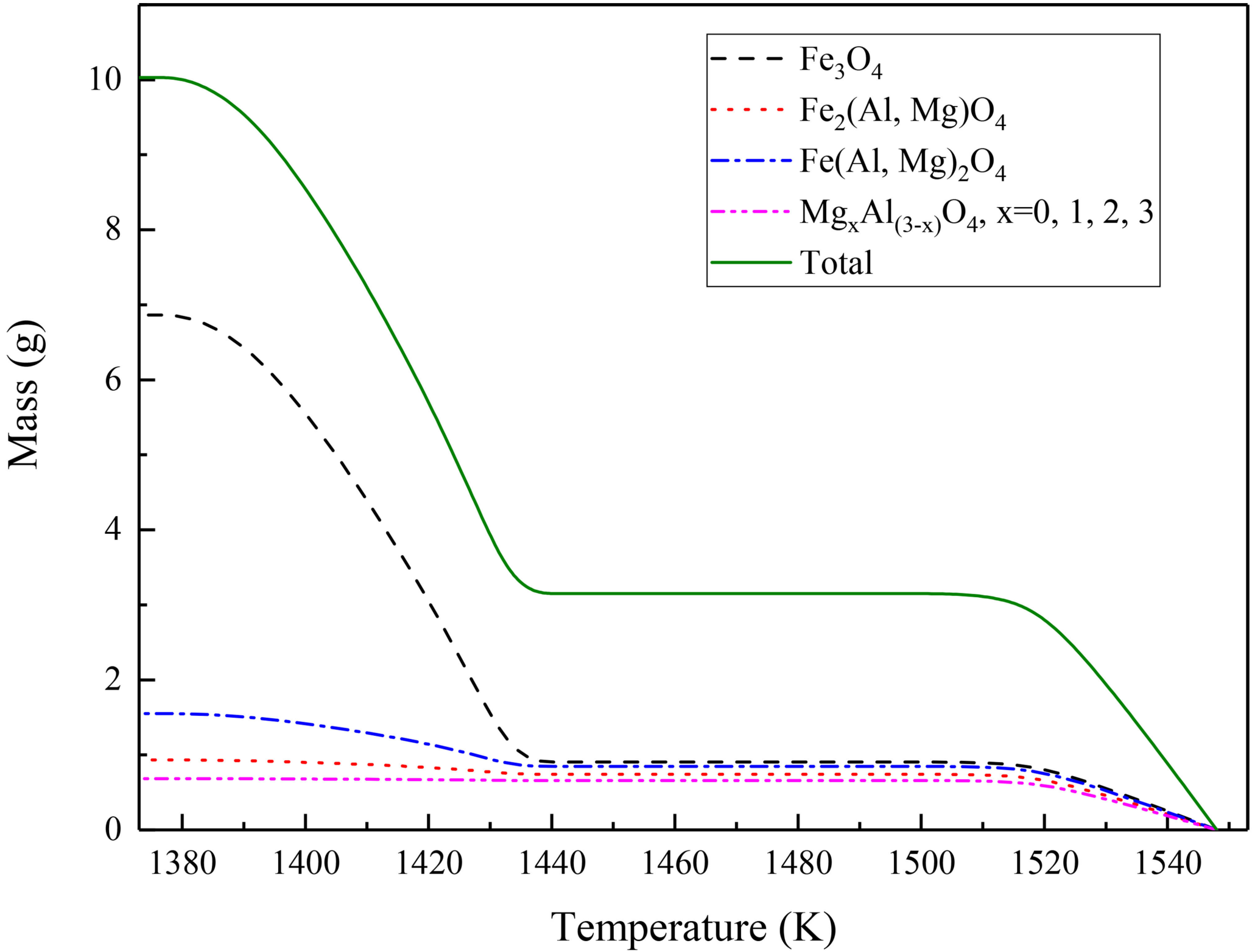
Fe3O4
Fe2(Al, Mg)O4
Fe(Al, Mg)2O4
MgxAl(3-x)O4, x=0, 1, 2, 3
Total
Mass (g)
Temperature (K)
0
2
4
6
8
10
1380
1400
1420
1440
1460
1480
1500
1520
1540

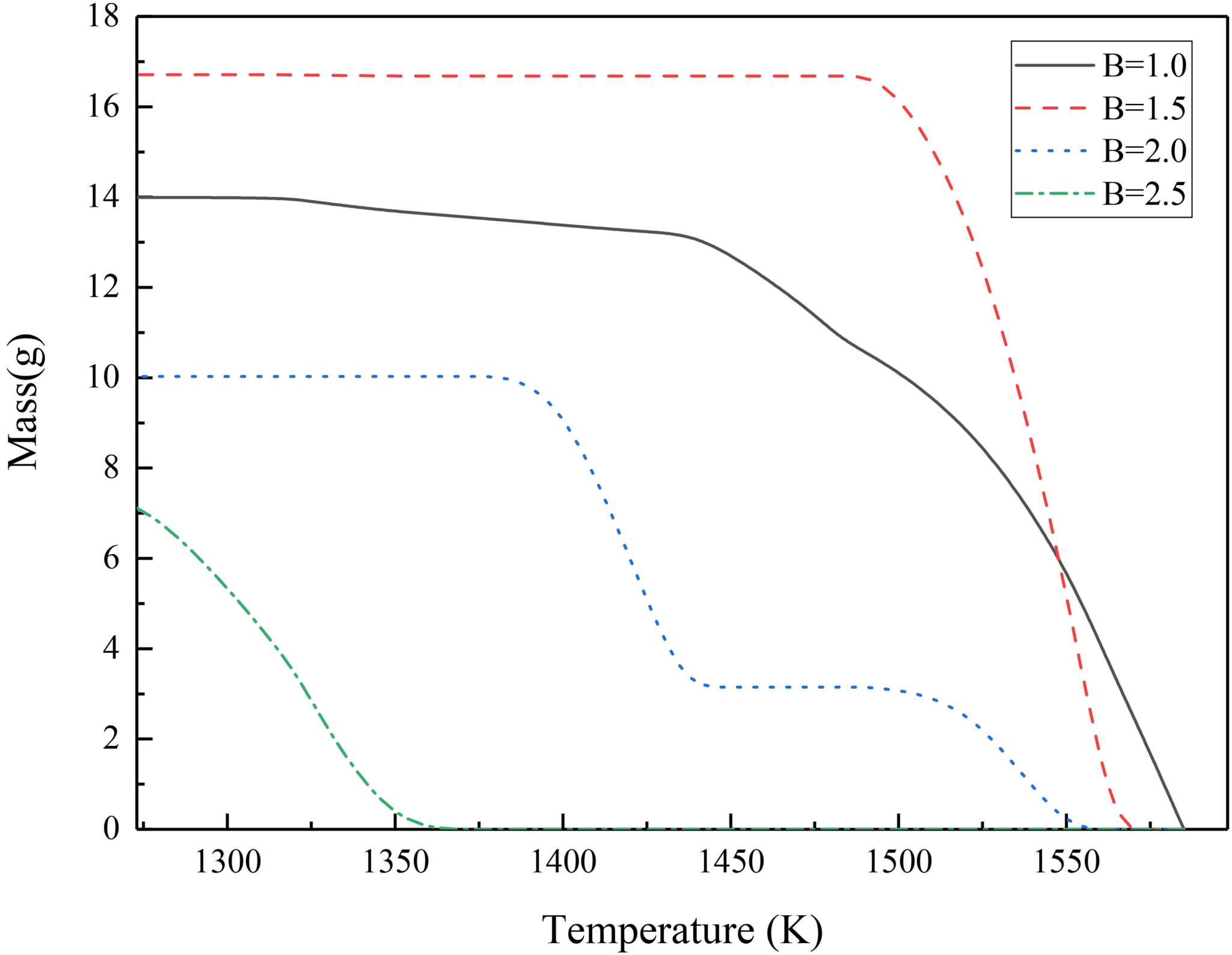
B=1.0
B=1.5
B=2.0
B=2.5
Mass(g)
Temperature (K)
0
2
4
6
8
10
12
14
16
18
1300
1350
1400
1450
1500
1550

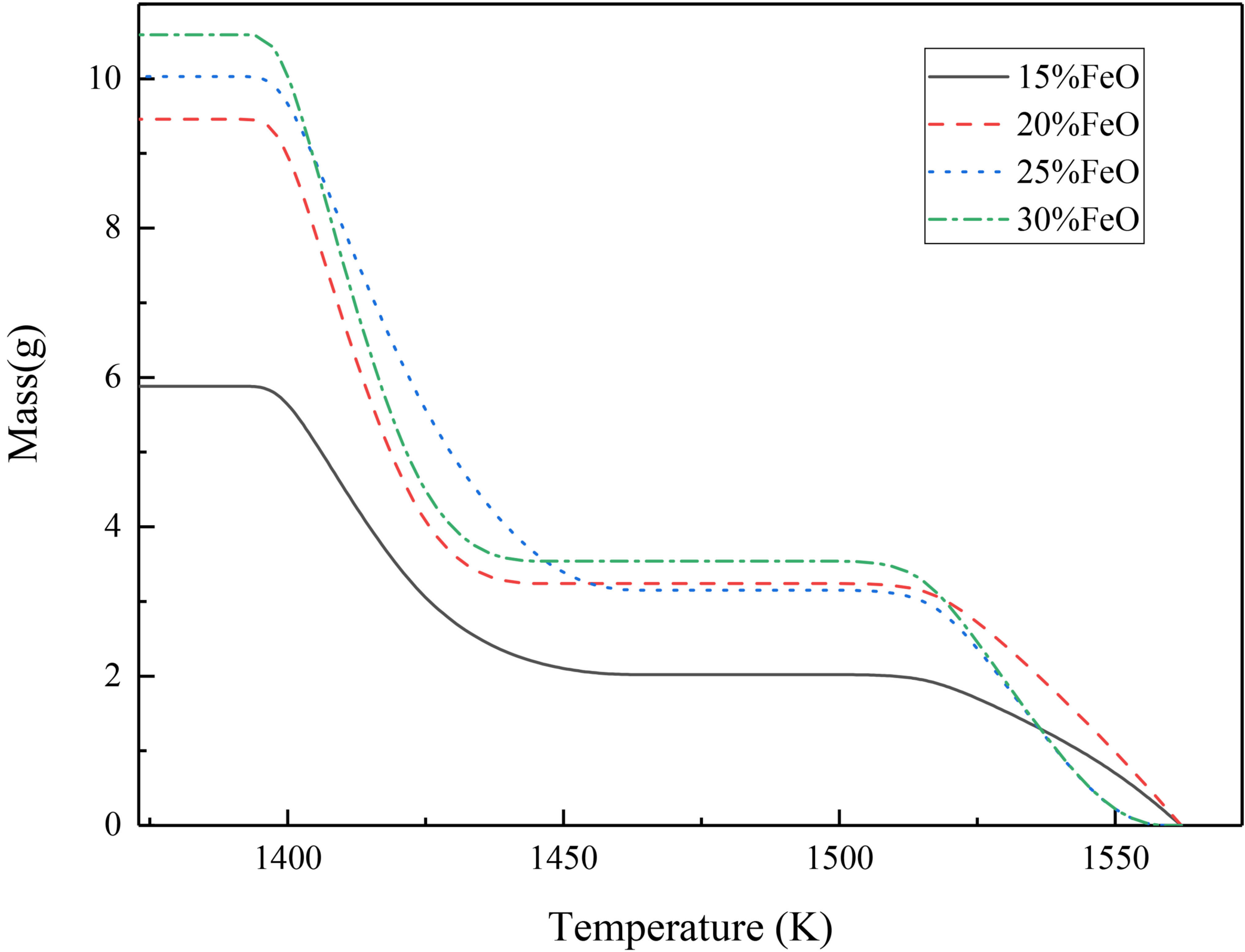
15%FeO
20%FeO
25%FeO
30%FeO
Mass(g)
0
2
4
6
8
10
1400
1450
1500
1550
Temperature (K)

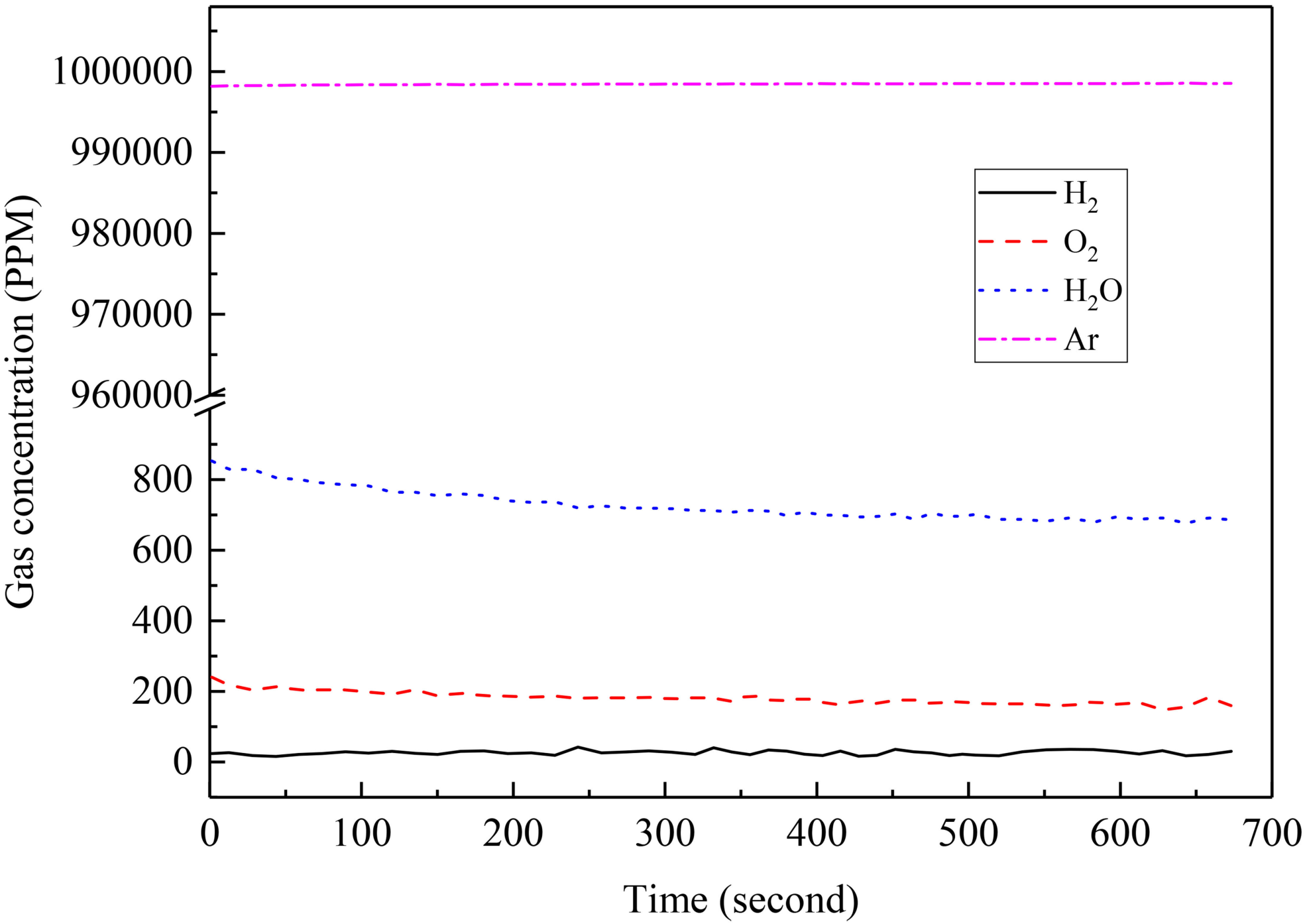
1000000
990000
980000
970000
960000
800
600
400
200
0
Gas concentration (PPM)
0
100
200
300
400
500
600
700
Time (second)
H2
O2
H2O
Ar

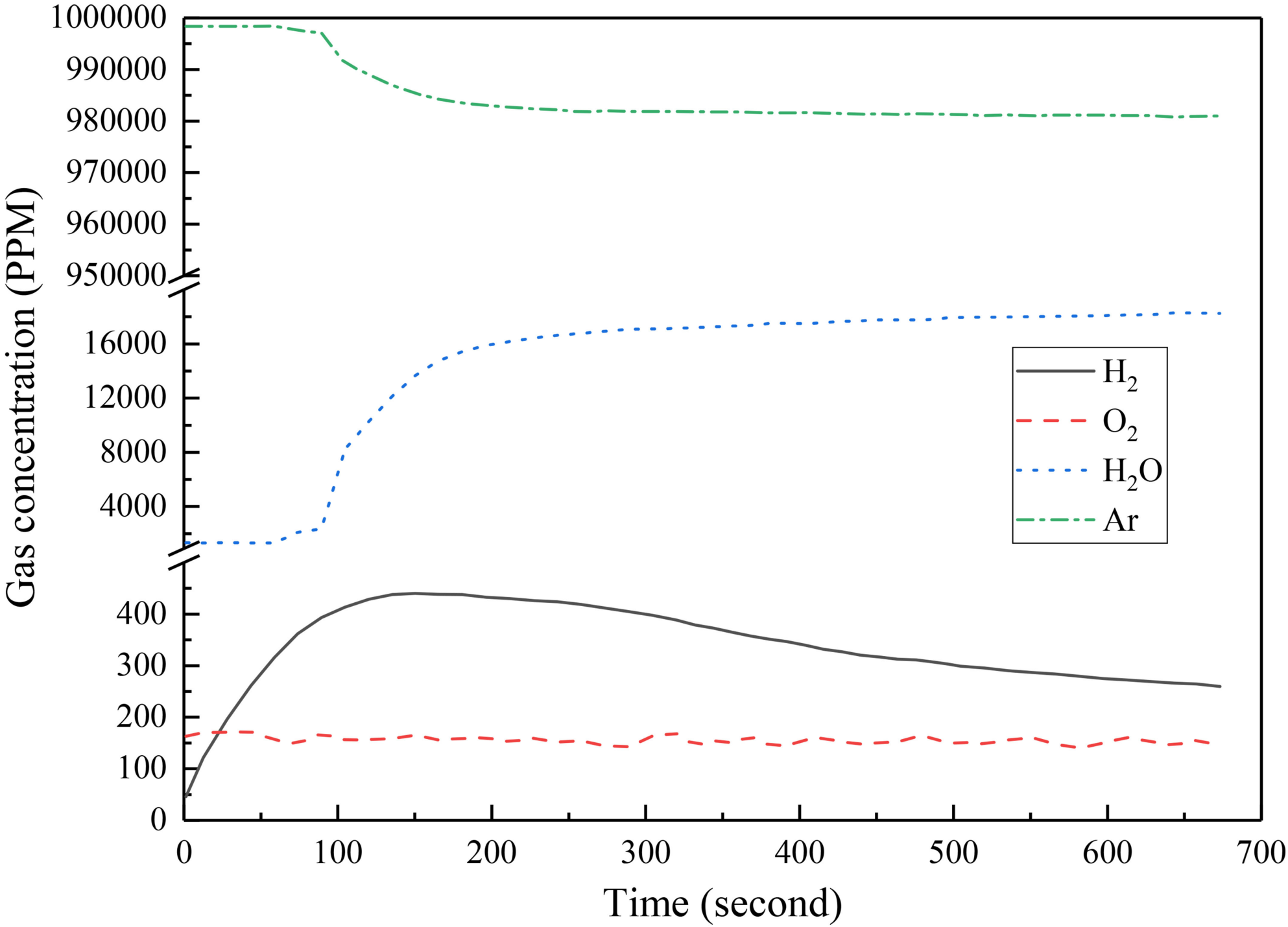
1000000
990000
980000
970000
960000
950000
16000
12000
8000
4000
400
300
200
100
0
Gas concentration (PPM)
0
100
200
300
400
500
600
700
Time (second)
H2
O2
H2O
Ar

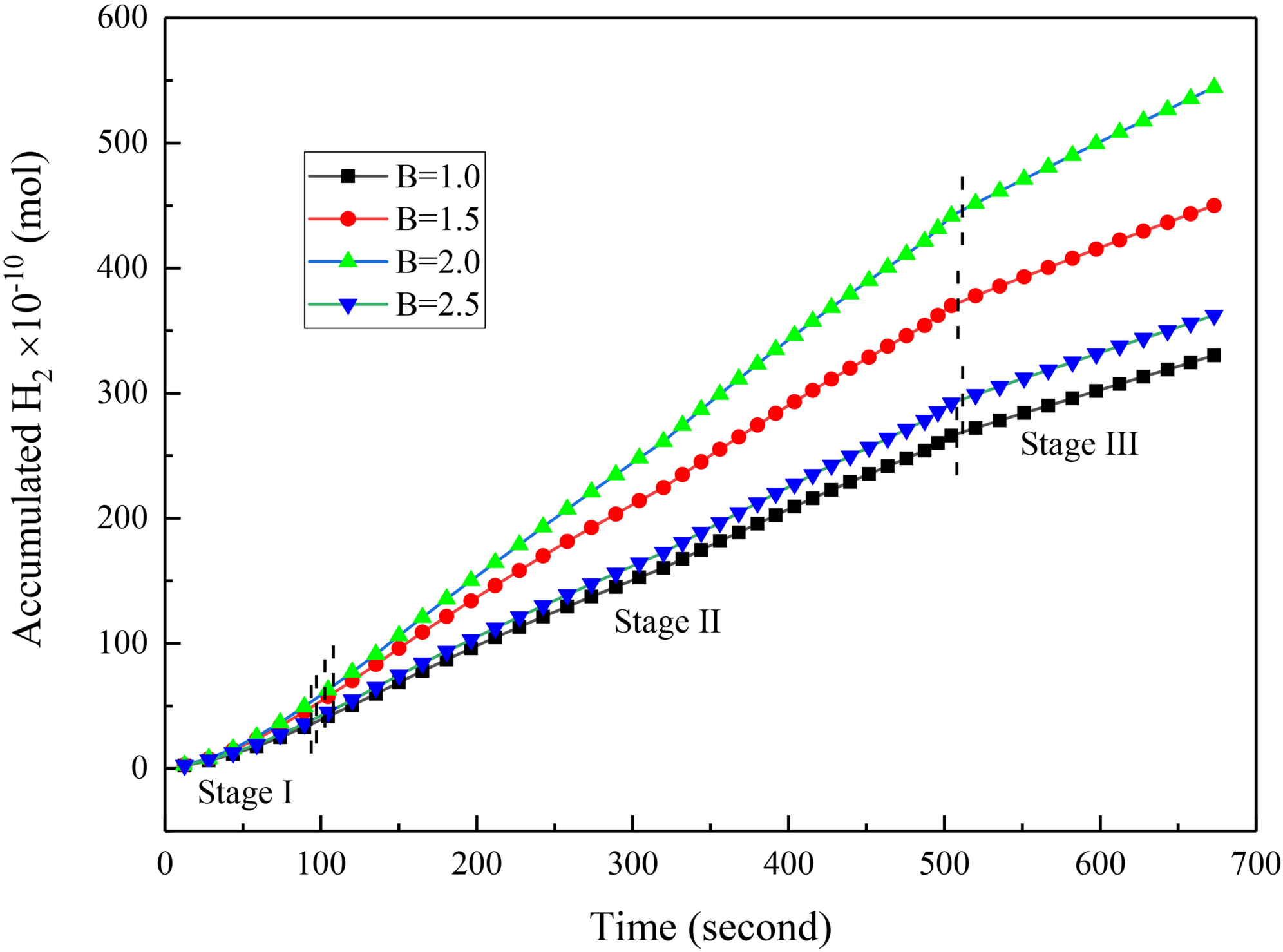
B=1.0
B=1.5
B=2.0
B=2.5
Stage I
Stage II
Stage III
Accumulated $H_2 \times 10^{-10}$ (mol)
Time (second)
600
500
400
300
200
100
0
0
100
200
300
400
500
600
700

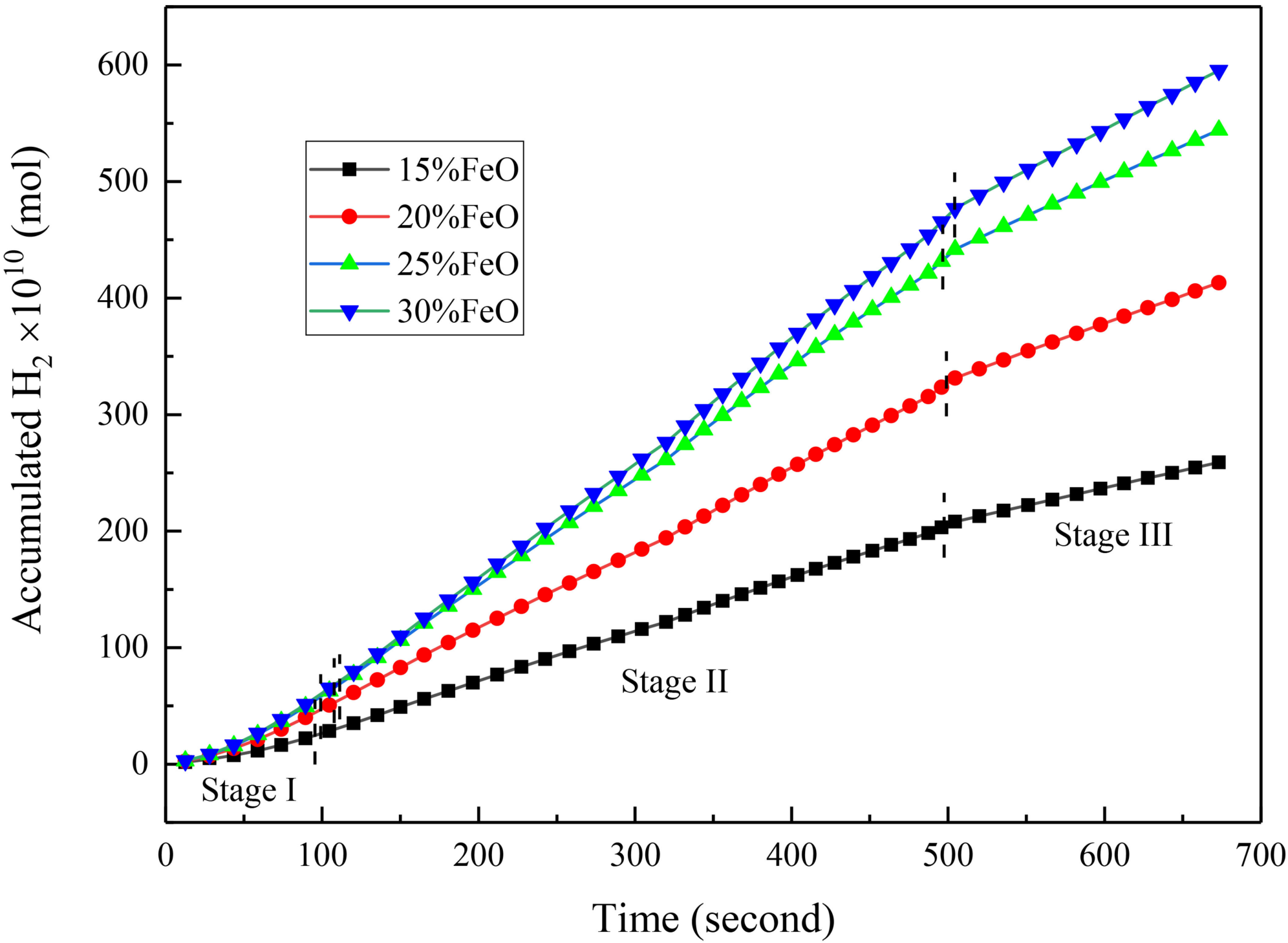
15%FeO
20%FeO
25%FeO
30%FeO
Stage I
Stage II
Stage III
Accumulated $H_2 \times 10^{10}$ (mol)
Time (second)
0
100
200
300
400
500
600
700

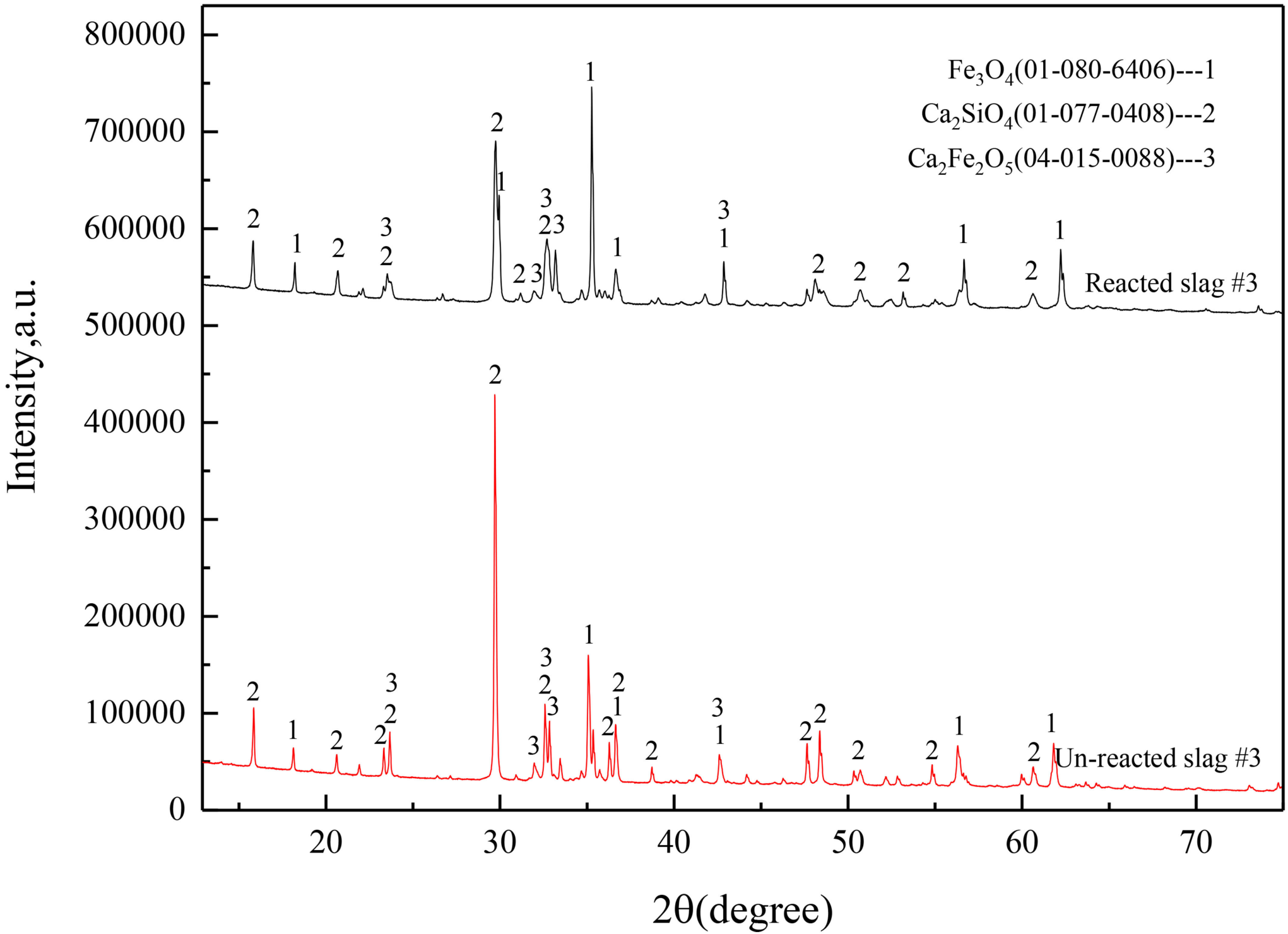
Fe3O4(01-080-6406)---1
Ca2SiO4(01-077-0408)---2
Ca2Fe2O5(04-015-0088)---3
Reacted slag #3
Un-reacted slag #3
Intensity,a.u.
2θ(degree)
800000
700000
600000
500000
400000
300000
200000
100000
0
20
30
40
50
60
70

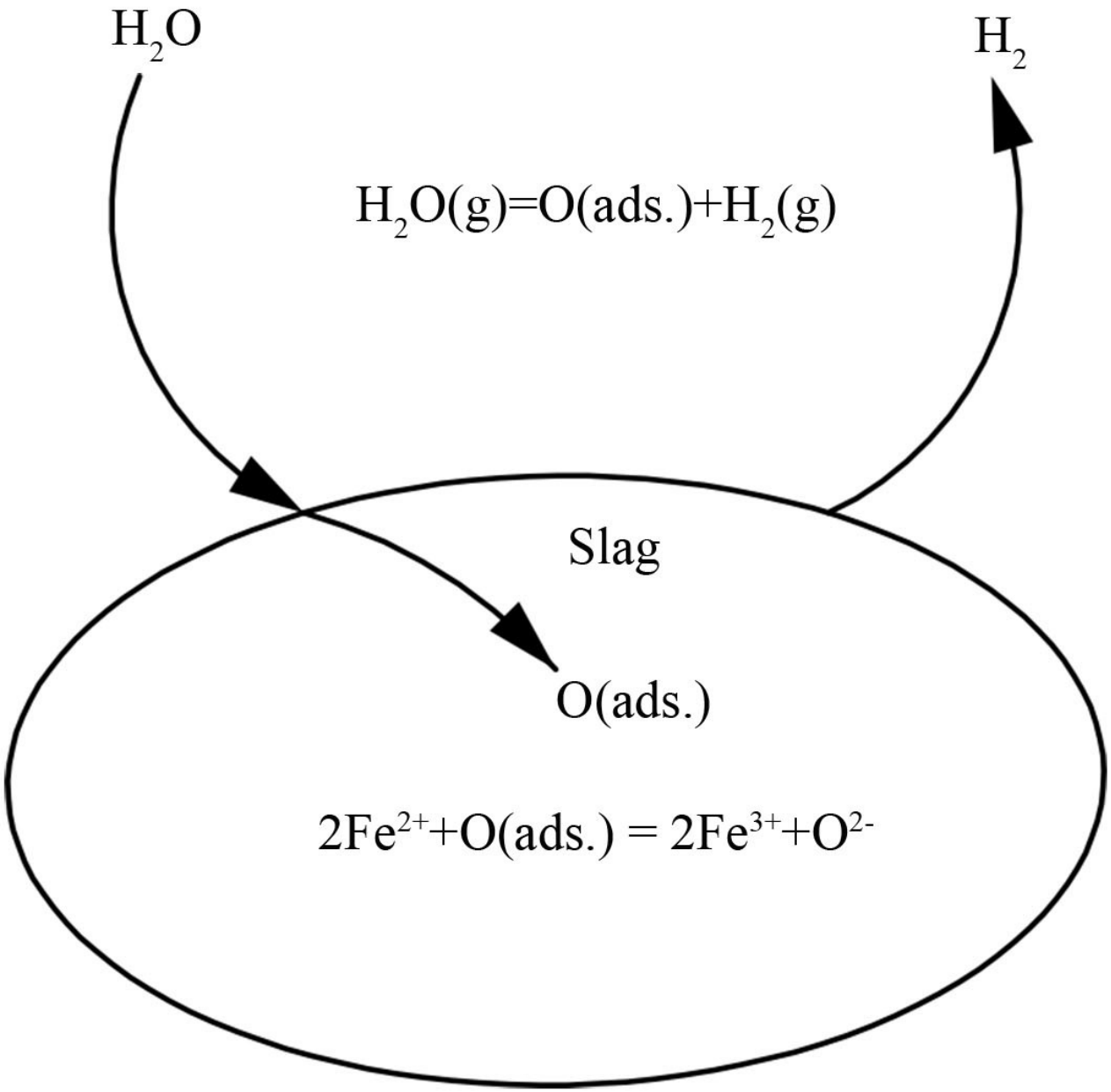

(1) H_2O decomposition

$H_2O(g) = O(ads.)+H_2(g)$

(2) FeO oxidization

$2Fe^{2+}+O(ads.) = 2Fe^{3+}+O^{2-}$

(3) Overall reaction

$H_2O(g)+2Fe^{2+} =2Fe^{3+}+H_2(g)+O^{2-}$

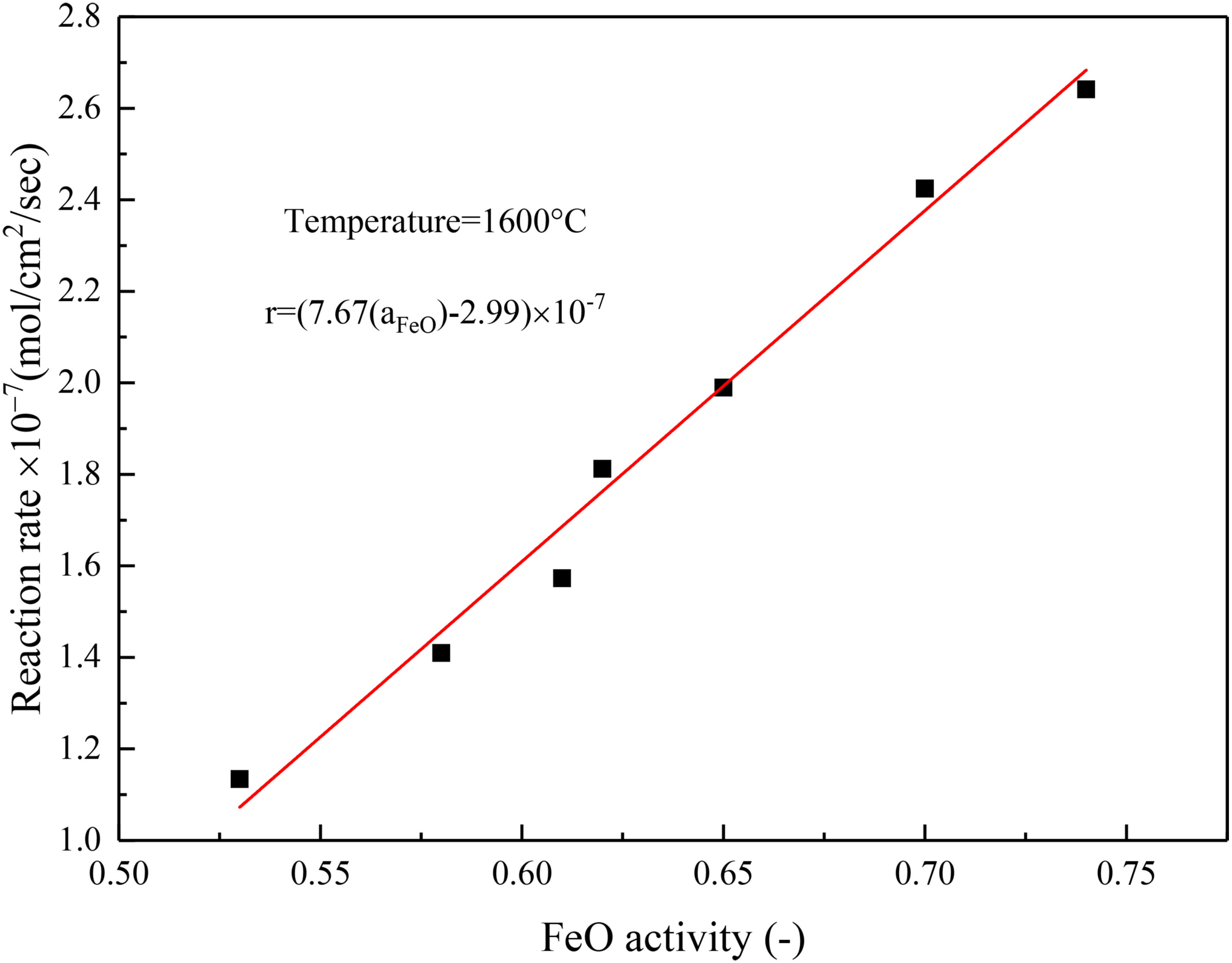
Temperature=1600°C
r=(7.67(a_FeO)-2.99)×10^-7
Reaction rate ×10^-7(mol/cm^2/sec)
FeO activity (-)
2.8
2.6
2.4
2.2
2.0
1.8
1.6
1.4
1.2
1.0
0.50
0.55
0.60
0.65
0.70
0.75

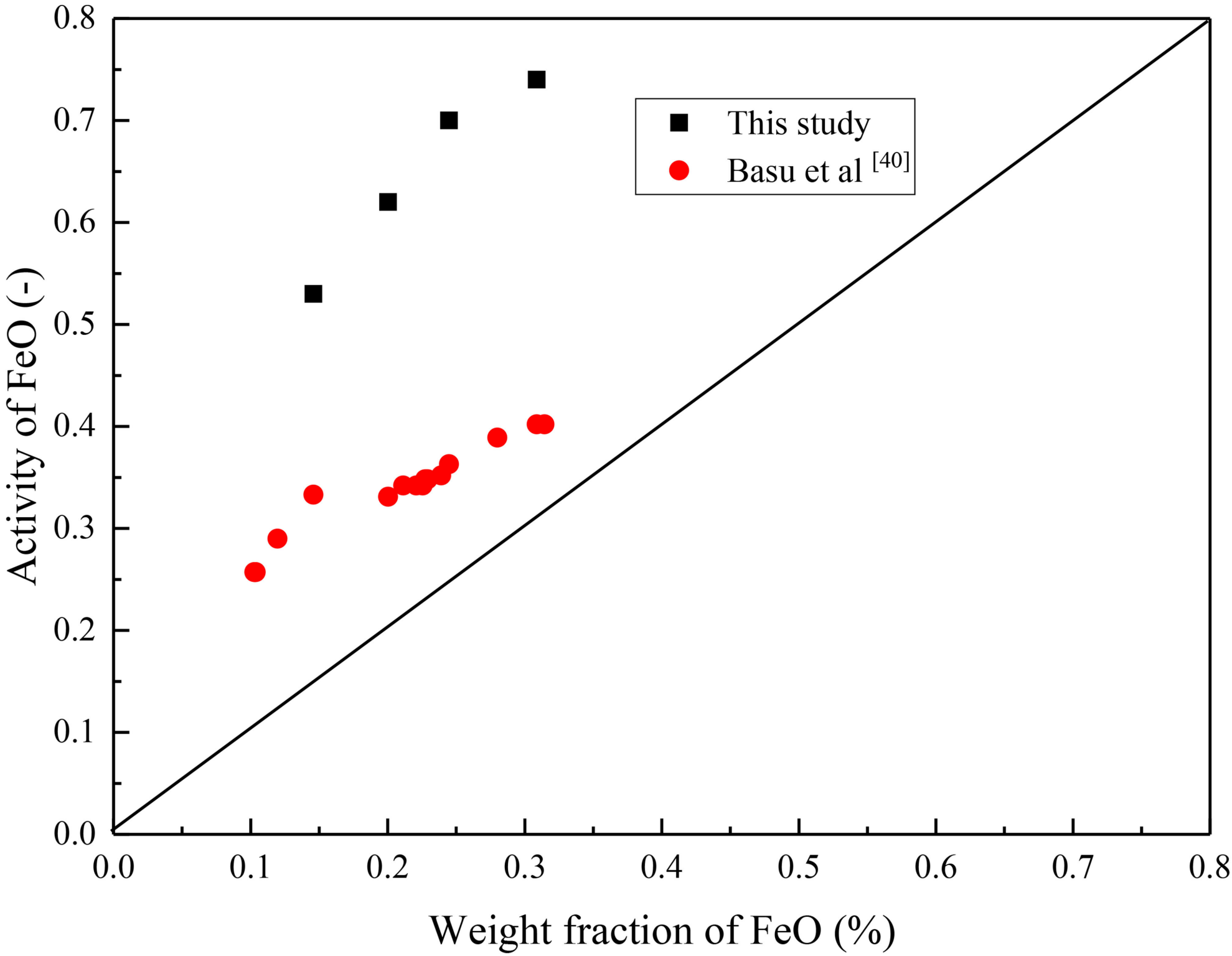
This study
Basu et al [40]
Activity of FeO (-)
Weight fraction of FeO (%)
0.0
0.1
0.2
0.3
0.4
0.5
0.6
0.7
0.8

$CaO - SiO_2 - FeO - MnO - Al_2O_3 - MgO - O_2$

CaO/Z (mol/mol) = 0.4, SiO_2/Z (mol/mol) = 0.2, FeO/Z (mol/mol) = 0.25, MnO/Z (mol/mol) = 0.05, Al_2O_3/Z (mol/mol) = 0.05, $Z=(CaO+SiO_2+FeO+MnO+Al_2O_3+MgO)$, 1 atm